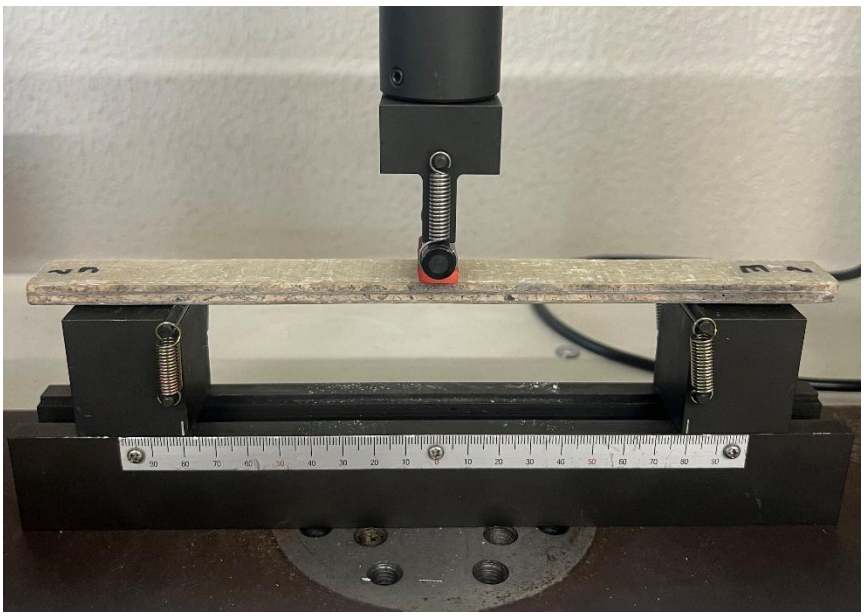

Analysis of Reinforced Cork Composite Sandwich Beams

SÉRGIO FILIPE MARQUES CAMPOS COSTA
(Licenciado em Engenharia Mecânica)

Dissertação para obtenção do grau de Mestre em Engenharia Mecânica, na Área de Especialização de Manutenção e Produção

Orientadores:
Doutor Afonso Manuel da Costa de Sousa Leite
Doutor Hugo Alexandre Freixial Argente dos Santos

Júri:
Presidente: Doutora Maria Amélia Ramos Loja
Vogais:
Doutora Maria Alexandra Sousa Rodrigues
Doutor Afonso Manuel da Costa de Sousa Leite

Dezembro de 2025

Analysis of Reinforced Cork Composite Sandwich Beams

SÉRGIO FILIPE MARQUES CAMPOS COSTA

(Licenciado em Engenharia Mecânica)

Dissertação para obtenção do grau de Mestre em Engenharia Mecânica, na Área de Especialização de Manutenção e Produção

Orientadores:

Doutor Afonso Manuel da Costa de Sousa Leite, ESTS/IPS
Doutor Hugo Alexandre Freixial Argente dos Santos, ISEL/IPL

Júri:

Presidente: Doutora Maria Amélia Ramos Loja, ISEL/IPL
Vogais:
Doutora Maria Alexandra Sousa Rodrigues, ISEL/IPL
Doutor Afonso Manuel da Costa de Sousa Leite, ESTS/IPS

Dezembro de 2025

Acknowledgements

As the author of this thesis, I'd like to thank to my supervisors, Dr. Afonso Leite and Dr. Hugo Santos for their support, guidance and suggestions during the project.

To Dr. Eiras, for providing the experimental specimens.

To Euroatlantic Airways, for providing me all the flexibility to attend the master's degree classes and exams.

To Airbus, for allowing me to balance my work time in accordance with the needs to perform the experimental tests of this study during working hours period.

To AEPS Europa for supporting me to finalize this project, by providing all the flexibility to allocate all the time possible on this project.

Finally, to my family and my girlfriend for their fundamental support to accomplish this milestone, without them I would not be capable to do so.

Thanks to you all.

Statement of integrity

I declare that this dissertation is the result of my personal and independent research. Its content is original, and all sources listed in the bibliographic references were consulted and are duly mentioned in the text. I further declare that all scientific and technical references relevant to the development of the work are duly cited and included in the bibliographic references.

The author

Assinado por: Sérgio Filipe Marques Campos Costa
Num. de Identificação: BI14655037
Data: 22-12-2025 17:46:10 +00:00

CHAVE MÓVEL

Lisbon, 22nd December 2025

Estudo de Vigas Sanduíche Compósitas com Núcleo em Cortiça Reforçada

Resumo

Considerando o contínuo aumento da utilização de materiais leves, biológicos e renováveis em todas as indústrias, a cortiça sendo um material que cumpre todos esses requisitos, mas que também oferece características mecânicas excecionais como a elevada resistência à compressão, mas também à tração, gera um enorme interesse para se testar e estudar o seu comportamento em aplicações de engenharia. Assim, este estudo tem como objetivo realizar um estudo experimental e numérico de vigas sandwich compósitas utilizando aglomerado de cortiça como núcleo, comparar os resultados com estudos anteriores e com outros materiais muito utilizados atualmente para discutir a sua viabilidade e limitações nas suas potenciais aplicações.

Foram utilizados vários provetes distribuídos em três tipos: T1, T2 e T3. Os provetes são feitos de compósito laminado usando resina epoxídica e tecido de fibra de vidro, nas peles, e núcleo de aglomerado de cortiça. Os diferentes tipos de viga apresentam também diferentes configurações de espessura das camadas nas peles e núcleos, tendo também camadas de fibra na zona do núcleo. Realizaram-se ensaios de flexão em três-pontos de acordo com a norma ASTM C393 para estudar o seu comportamento mecânico, calcular a sua rigidez à flexão, resistência ao corte e outras propriedades relevantes como a tensão de flexão nas peles, tensão critica ao corte do núcleo e a rigidez ao corte da sandwich.

Um estudo numérico com base na análise de elementos finitos de um modelo 2D desenvolvido no software Ansys, foi feito para simular o comportamento dos provetes no regime linear elástico e verificar o resultado experimental. Os resultados numéricos afastam-se dos experimentais no que concerne à deformada, mas há uma correlação razoável em termos de gráfico de força-deslocamento no regime linear elástico.

Palavras-Chave: Aglomerado de Cortiça, Vigas Sanduiche Compósitas, Análise por Elementos Finitos, Rigidez à flexão, Resistência ao Corte

Analysis of Reinforced Cork Composite Sandwich Beams

Abstract

Considering the continuous increase in the use of lightweight, biological, and renewable materials across all industries, cork—being a material that meets all these requirements while also offering exceptional mechanical characteristics such as high resistance to compression as well as to tension—generates significant interest for testing and studying its behavior in engineering applications. Thus, this study aims to carry out an experimental and numerical investigation of composite sandwich beams using cork agglomerate as the core, compare the results with previous studies and with other materials widely used today, and discuss their feasibility and limitations in potential applications.

Several specimens were used, distributed into three types: T1, T2, and T3. The specimens are made of laminated composite, using epoxy resin and glass fiber fabric for the skins, and a cork agglomerate core. The different beam types also present different configurations of skin and core thicknesses and include fiber layers in the core region as well. Three-point bending tests were performed according to ASTM C393 to study their mechanical behavior, calculate their flexural stiffness, shear strength, and other relevant properties such as bending stress in the skins, critical shear stress of the core, and the shear stiffness of the sandwich structure.

A numerical study based on finite element analysis of a 2D model developed in Ansys software was conducted to simulate the behavior of the specimens in the linear elastic regime and to verify the experimental results. The numerical results deviate from the experimental ones with respect to the deformed shape; however, there is a reasonable correlation in terms of the force–displacement curve in the linear elastic regime.

Keywords: Composite Sandwich Beams, Reinforced Cork, Experimental Analysis, Finite Element Analysis, Flexural Stiffness, Shear Strength

Nomenclature

Roman Alphabet

T1 Type 1 specimen

T2 Type 2 specimen

T3 Type 3 Specimen

2F 2 plies of reinforced fiberglass fabric

4F 4 plies of reinforced fiberglass fabric

5F 5 plies of reinforced fiberglass fabric

1C 1 Cork core layer

d Sandwich thickness

b Sandwich width

L Span length

Mf Mass fraction

Mm Matrix mass

Vf Volume fraction

Vm Volume matrix

P load

U Sandwich beam rigidity

D Flexural stiffness

E_x Elastic modulus x-direction

E_y Elastic modulus y-direction

E_z Elastic modulus z-direction

G_{xy} shear modulus longitudinal direction

G_{yz} shear modulus transversal direction

G_{xz} shear modulus z-direction

h_f *facing thickness*

G_c *core shear modulus*

Greek Alphabet

σ_{cr} critical facing wrinkling stress

τ core shear stress

v_{xy} Poisson ratio longitudinal direction

v_{yz} Poisson ratio transversal direction

v_{xz} Poisson ratio in z-direction

σ_{cshear} critical shear stress

t_f face sheet thickness

τ Core shear stress

Δ_{3PB} Displacement on 3PB test

Siglum

ASTM American Society for Testing and Materials

FEA Finite Element Analysis

FEM Finite Element Method

3PB Three-point Bending

4PB Four-point Bending

Table of Contents

1 INTRODUCTION 1

1.1 Present Study Relevancy 1

1.2 Goal of the Study 2

1.3 Document Structure 2

2 STATE-OF-THE-ART 3

2.1 Composite material definition 3

2.2 Classification and Characteristics of Composite Materials 3

2.2.1 Unidirectional and bidirectional fiber composite materials 4

2.2.2 Fibers 6

2.2.3 Matrix 7

2.2.4 Laminated Composite Materials 8

2.3 Sandwich composite structures 10

2.3.1 Core Material 12

2.3.2 Facings 13

2.3.3 Matrix 14

2.4 Cork 14

2.4.1 Cork Harvesting 16

2.4.2 Macroscopic Analyses 17

2.4.3 Microscopic Analysis 18

2.4.4 Mechanical Analyses 19

2.5 Sandwich Beam Experimental Analysis 22

2.6 Numerical Analysis of Sandwich Beams 24

2.7 Sandwich Beam Failure Modes 25

2.7.1 Facing yielding/fracture 26

2.7.2 Facing Wrinkling or local buckling 26

2.7.3 Core failure or fracture 27

3 EXPERIMENTAL ANALYSIS 28

3.1 Sandwich Specimens Manufacturing 28

3.2 Experimental Methodologies 32

3.2.1 Verification of conformity with ASTM Standard Test C 393-00 33

3.3 Experimental Tests Set-up 34

3.4 Experimental Results and Discussion 36

3.5 Flexural Properties Calculation 40

3.5.1 Facing bending stress 40

3.5.2 Sandwich beam shear rigidity 41

3.5.3 Ultimate Sandwich core shear stress 42

3.5.4 Sandwich beam flexural Stiffness *43*
3.5.5 Sandwich beam 3PB Deflection *44*
4 NUMERICAL ANALYSIS **46**
4.1 NUMERICAL MODEL 46
4.1.1 Epoxy/Fiberglass composite material properties *46*
4.1.2 Cork core material properties *47*
4.1 NUMERICAL RESULTS 49
5 FAILURE MODES ANALYSIS **52**
5.1 T1 SPECIMENS ANALYSIS 52
5.2 T2 SPECIMENS ANALYSIS 53
5.3 T3 SPECIMENS ANALYSIS 53
6 COMPARISON WITH OTHER MATERIALS **55**
7 CONCLUSIONS AND FUTURE WORKS **57**
7.1 CONCLUSIONS 57
7.2 FUTURE WORKS 58
REFERENCES **60**
APPENDIX 1 - ANSYS NUMERICAL FEM MODEL 2D – T1 SPECIMEN'S **63**
APPENDIX 2 - ANSYS NUMERICAL FEM MODEL 2D – T2 SPECIMEN'S **72**
APPENDIX 3 - ANSYS NUMERICAL FEM MODEL 2D – T3 SPECIMEN'S **85**

List of Figures

Figure 2.1 - Unidirectional composite material load directions [1]. 4
Figure 2.2- Unidirectional and bidirectional oriented materials [8]. 5
Figure 2.3 - Fabric Plain and Satin weaves [8]. 5
Figure 2.4 - Comparison between tape and fabric products [8]. 6
Figure 2.5 - Stress-strain curves of reinforced fiber composite material and comparison with respective fiber and matrix separated [2]. 7
Figure 2.6 - Quasi-isotropic composite material layup [8]. 8
Figure 2.7 - Laminate composite scheme [2]. 9
Figure 2.8 - Different material distribution on a Boeing 787 Aircraft structure [5]. 10
Figure 2.9 - Honeycomb Sandwich panel [9]. 11
Figure 2.10 - Stiffness/weight with thickness increase of a typical composite sandwich material [6]. 12
Figure 2.11 - Comparison between I-beam and sandwich composite beam [11]. 12
Figure 2.12 - Cork section cut in the tree [14]. 15
Figure 2.13 – Production of cork per country [15]. 15
Figure 2.14 - Cork being removed from the oak tree [15]. 16
Figure 2.15 - Stack of cork after harvesting [15]. 17
Figure 2.16 - Section cut of a cork sample [19]. 18
Figure 2.17 - Cork cellular disposition in cork: a) radial section and b) tangential section [12]. 18
Figure 2.18 - Cork Cell wall scheme: (T) tertiary wall, (S) Secondary wall, (W) Waxes or polymers and suberin, (P) Primary wall, (M)Medium lamella, (Po) Pore [12]. 19
Figure 2.19 - Nominal Stress-Strain Curve of cork in compression [21]. 19
Figure 2.20 - stress-strain curve of cork obtained on a quasi-static compressive test on specimens C3, C6 and C8 [22]. 20
Figure 2.21 - Tensile load-displacement curve of cork [22]. 21
Figure 2.22 - Comparison of Cork and other materials [23]. 21
Figure 2.23 - Sandwich structure 3PB stresses [6]. 22
Figure 2.24 - Load-Displacement curve of cork core made sandwich specimens [25]. 23
Figure 2.25 - Load-Displacement curve of honeycomb core made sandwich specimens [25]. 23
Figure 2.26 - Sandwich beams typical failure modes: (a) for facing fracture, (b) for the core failure examples and (c) and (d) for local buckling [11]. 25
Figure 2.27 – T3 Specimen Face Wrinkling 27
Figure 3.1 - Experimental Sandwich Composite after mold removal. 29
Figure 3.2 - T1 (5F/1C/5F) Sandwich Specimen. 29
Figure 3.3 - T2 (4F/1C/2F/1C/4F) Sandwich Specimen. 29

FIGURE 3.4 - T3 (5F/1C/5F/1C/5F) SANDWICH SPECIMEN..... 30
FIGURE 3.5- THREE-POINT BENDING TEST SPECIMEN SKETCH [25]..... 33
FIGURE 3.6- SINGLE-POINT LOAD ON A THREE-POINT FLEXURAL TEST [32]..... 34
FIGURE 3.7 – UNIVERSAL TESTING MACHINE WITH 3 POINT BENDING TEST FIXTURE MOUNTED..... 35
FIGURE 3.8- SPECIMEN POSITIONING..... 35
FIGURE 3.9 - TRIAL TEST WITHOUT PROTECTIVE RUBBER..... 36
FIGURE 3.10 - SPECIMENS TIME TO RUPTURE..... 37
FIGURE 3.11 - TYPICAL CORK AGGLOMERATE LOAD-DISPLACEMENT CURVE [36]..... 38
FIGURE 3.12 - EXPERIMENTAL LOAD-DISPLACEMENT CURVES FOR T1 SPECIMENS..... 38
FIGURE 3.13 - EXPERIMENTAL LOAD-DISPLACEMENT CURVES FOR T2 SPECIMENS..... 39
FIGURE 3.14 - EXPERIMENTAL LOAD-DISPLACEMENT CURVES FOR T3 SPECIMENS..... 39
FIGURE 4.1 - T1 SPECIMEN MESHING SETTING..... 48
FIGURE 4.2 - THREE-POINT BENDING NUMERICAL TEST BODY DIAGRAM..... 48
FIGURE 4.3 - THREE-POINT BENDING NUMERICAL RESULT OF SPECIMEN T1..... 49
FIGURE 4.4 - THREE-POINT BENDING NUMERICAL RESULT OF SPECIMEN T2..... 50
FIGURE 4.5 - THREE-POINT BENDING NUMERICAL RESULT OF SPECIMEN T3..... 50
FIGURE 4.6 - T1 EXPERIMENTAL AND NUMERICAL RESULTS..... 50
FIGURE 4.7 - T2 EXPERIMENTAL AND NUMERICAL RESULTS..... 51
FIGURE 4.8 - T3 EXPERIMENTAL AND NUMERICAL RESULTS..... 51
FIGURE 5.1 - T1 SPECIMEN CORE CRACK..... 52
FIGURE 5.2 - T2 SPECIMEN CORE FAILURE..... 53
FIGURE 5.3 -T3 SPECIMEN CRUSHED FACING..... 54

List of Tables

TABLE 2.1 - COMMON FIBER PROPERTIES [1]. 8
TABLE 2.2 - COMMONLY USED FIBERS IN AEROSPACE INDUSTRY [4]. 10
TABLE 2.3- COMMON CORE MATERIALS AND THEIR PROPERTIES [11]. 13
TABLE 3.1 - DIMENSIONS OF THE THREE TYPES OF SPECIMENS. 30
TABLE 3.2 - REINFORCED FIBER-GLASS MASS AND VOLUME FRACTIONS. 32
TABLE 3.3 - EXPERIMENTAL RESULTS OF LOAD AT RUPTURE, TIME AT RUPTURE AND SPEED. 37
TABLE 3.4 - EXPERIMENTAL DEFLECTION AT RUPTURE. 40
TABLE 3.5 – MAXIMUM FACING BENDING STRESS. 41
TABLE 3.6 - SANDWICH BEAM SHEAR RIGIDITY. 42
TABLE 3.7 - SPECIMENS CORE MAXIMUM SHEAR STRESS. 43
TABLE 3.8 - SPECIMENS AVERAGE FLEXURAL STIFFNESS. 44
TABLE 3.9 - THEORETICAL SPECIMEN DEFLECTION. 45
TABLE 4.1 - EPOXY/FIBER-GLASS LAMINATE MATERIAL PROPERTIES. 47
TABLE 4.2 - CORK CORE MATERIAL PROPERTIES [38]. 47
TABLE 4.3 - LINEAR ELASTIC REGIME MAXIMUM LOADS. 49
TABLE 6.1 – FLEXURAL TESTS GLOBAL RESULTS. 55
TABLE 6.2 - COMPARISON BETWEEN T1, T2 AND T3 RESULTS WITH DIFFERENT SANDWICH BEAM RESULTS FROM OTHER STUDIES. 56

1 Introduction

1.1 Present Study Relevancy

The use and development of new composite materials play a key role across a wide range of industries and engineering applications due to the vast diversification of material combinations that can be achieved. This versatility enables the conjunction of mechanical, thermal, and physical properties to meet specific performance requirements, making composites an attractive solution for structural and functional purposes. In particular, the development of advanced composite materials that have progressively replaced traditional metallic components represents a significant leap in efficiency, as they provide substantial reductions in weight while maintaining or even improving mechanical performance and durability in demanding environments.

Composite sandwich structures are one such innovation. Their design conceptually resembles the typical “I”-beam, where the outer skins primarily resist tensile and compressive stresses, while the lightweight core sustains shear stresses and prevents buckling. By employing a low-density core material, these structures achieve an exceptionally high stiffness-to-mass ratio, allowing them to withstand considerable shear and flexural loads with a dramatically reduced overall weight. Such properties have led to their widespread use in aerospace, marine, automotive, and civil engineering applications where structural efficiency and energy absorption are critical. The use of cork as a core material in sandwich composites has recently attracted growing attention due to its unique natural characteristics. Cork exhibits remarkable compressive strength, high resilience under impact and cyclic loading, and an exceptional ability to recover its shape after deformation. Moreover, it offers excellent thermal and acoustic insulation properties, low permeability to liquids and gases, and strong damping behavior. From an environmental perspective, cork is a renewable, biodegradable, and recyclable material due to the fact that it can be transformed into a recycled cork agglomerate, aligning with the increasing demand for sustainable engineering solutions. These combined attributes make cork agglomerate an appealing candidate for lightweight structural cores, promoting both performance and ecological responsibility in modern composite design.

1.2 Goal of the Study

The main goal of this study is to perform an experimental and numerical analysis to several sandwich composite beam specimens by submitting the specimens to several 3PB bending tests, observe the performance of the different specimens, compare it to the expected results from literature and previous studies, to be able to discuss and reach conclusions about its potential and limitations for applications and future improvements.

1.3 Document Structure

Chapter 2 of this thesis presents a state-of-the-art review of cork as a material, sandwich composite structures and previous experimental and numerical studies of cork utilization as the core of sandwich composite structures.

Chapter 3 presents the experimental analysis, on which the specimens manufacturing procedure is included, the ASTM C393 introduction, the three-point bending testing, results obtained and properties calculation.

Chapter 4 presents the numerical analysis carried out by simulating a 2D Finite Element Model on which the maximum load verified on the experimental tests was used for each specimen, to check the agreement of the FEM solution with the experimental result for the linear elastic regime of the test.

Chapter 5 addresses the results obtained, more focused on each specimens behaviour and failure modes, comparing with the literature and making relevant considerations.

Chapter 6 gives an overall results visibility and comparison with previous studies made on sandwich composite beams, under 3PB testing with cork agglomerates on its core, but also with commonly used standard materials.

On chapter 7, several conclusions are presented to summarize the study overall results, important considerations, issues that were noticed and lessons learned. There are also made several suggestive further works that can be done in order to add more relevant information to the existent study, methods to test the sandwich beams in a more accurate and exhaustive way in order to get a more complete study, delivering more reliable and useful results.

2 State-of-the-Art

2.1 Composite material definition

Composite materials are characterized by the combination of various materials with different properties, aiming to get a product with properties that cannot be obtained using a single structure material [1]. This idea is used by humans since thousands of years, for example when the first houses were build using mud and wood combined to get stronger walls and roofs when comparing to the construction using a single material for the same purpose.

Basically speaking, composite materials can be described by a combination of different materials that do not dissolve with each other. This combination is then a macroscopic merging of two or more materials using another material that works as bonding material, so-called matrix [2]. The same cannot be verified on metal alloys, as those are the result of a microscopic relation between different materials, so metal alloys are not classified as a composite material. The result of a manufactured composite material can vary on its constituents, the percentage of each constituent, geometry and the way the different constituents are distributed [3]. Composite materials allow the possibility of using different materials, its amount, layer orientation and building techniques. Nowadays, composite materials are used largely in all industries worldwide, as the technology is revealing new refined materials which represent improvements on structures performance and new efficient engineering purposes.

2.2 Classification and Characteristics of Composite Materials

Composite materials are generally categorized into four types: (i) Fiber composites, which consist of the use of fibers in a matrix; (ii) Laminated composites, which consist of the build-up of layers of different materials; (iii) Particulate composites, which consist of the use of particles of a material on a matrix [1]. Fibers can be sometimes made of thousands of filaments in a scale of micrometers, known by its high length-to-diameter

ratio, and matrix is the material responsible to hold the fiber in place and distribute the loads within the material and forming a resultant product as illustrated on figure 2.1. In order to determine the best suitable material for a particular stiffness and/or strength for a particular structural application, the load directions on a composite material and its fiber orientation are one the most relevant selection criteria [1-7].

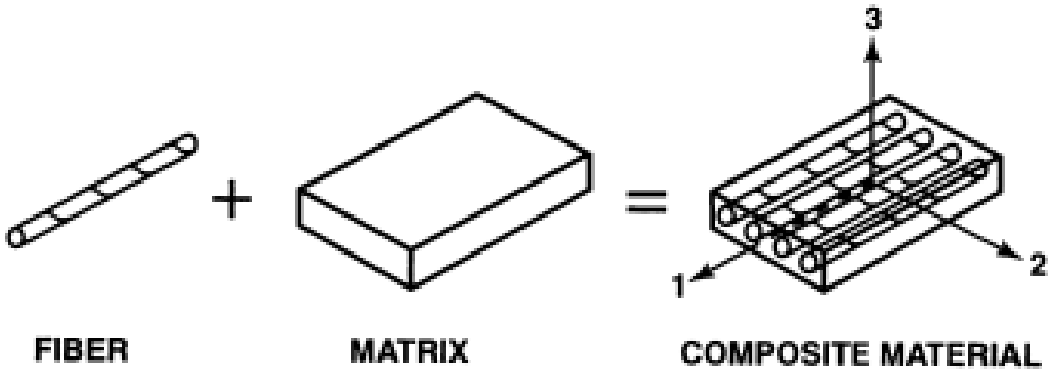

Figure 2.1 - Unidirectional composite material load directions [1].

2.2.1 Unidirectional and bidirectional fiber composite materials

A composite material is dependent on the fiber orientation as its structural behaviour will differ on different directions. A typical industrial fiber composite is illustrated in figure 2.1, showing the orientation of loads on a unidirectional composite material, presenting x-direction as (1), y-direction (2) and z-direction (3).

On a composite material, fibers are the load-carrying agent having the main strength and stiffness on its direction, therefore, its orientation should be in the direction of the loads. An example of a composite material with unidirectional orientation is the Pre-impregnated tape, which is widely used on aerospace industry, is made by the impregnation of a fiber (strands) into a hot melted resins using an impregnation machine at a high temperature and pressure, resulting on a high strength product in the fiber direction using the matrix (resin in this case) with the purpose of supporting and holding the fiber as well as distributing the loads along the fibers and between them.
The Bidirectional orientation of the fibers also known as fabric constructions, provides more flexibility either for a different shapes of products then tape or for its capability to

suit on applications that are under longitudinal (x-direction) and transverse direction (y-direction) as described in figure 2.2 below.

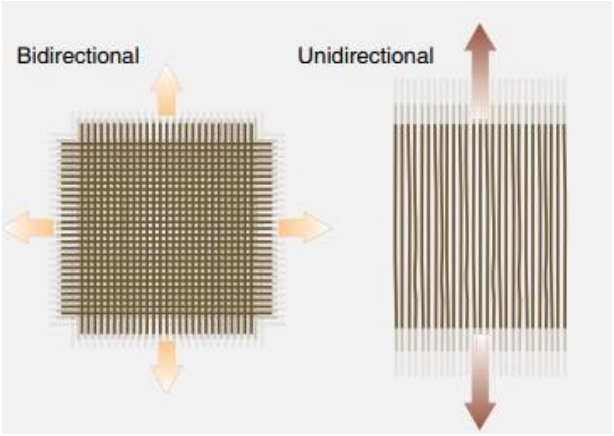

Figure 2.2- Unidirectional and bidirectional oriented materials [8].

Fabric products can be also characterized to use reinforcement tows that are woven between themselves called weaving process, of which the most common woven configurations are the satin or plain weaves as shown on figure 2.3. With this technique, the fabric product has the advantage to save weight due to less resin used for impregnation and keeping the fiber orientation which makes woven fabric products a great solution for many aerospace structures applications [6-8].

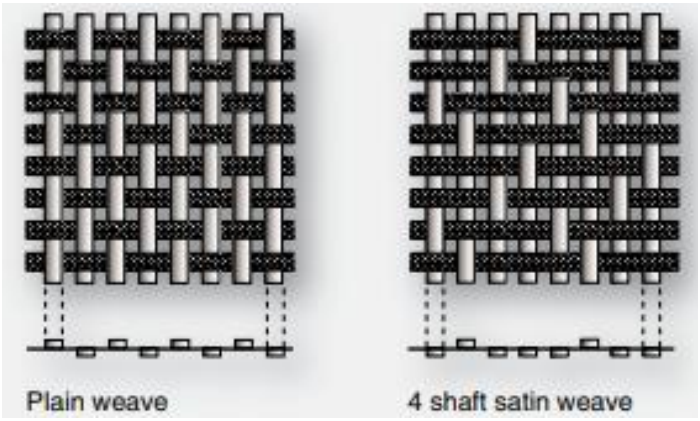

Figure 2.3 - Fabric Plain and Satin weaves [8].

Figure 2.4 shows the comparison between a tape product (unidirectional) and a fabric product (bidirectional), on which the individual tows of a tape product can be seen aligned in parallel and the fabric are buildup with a bidirectional and in a weave configuration.

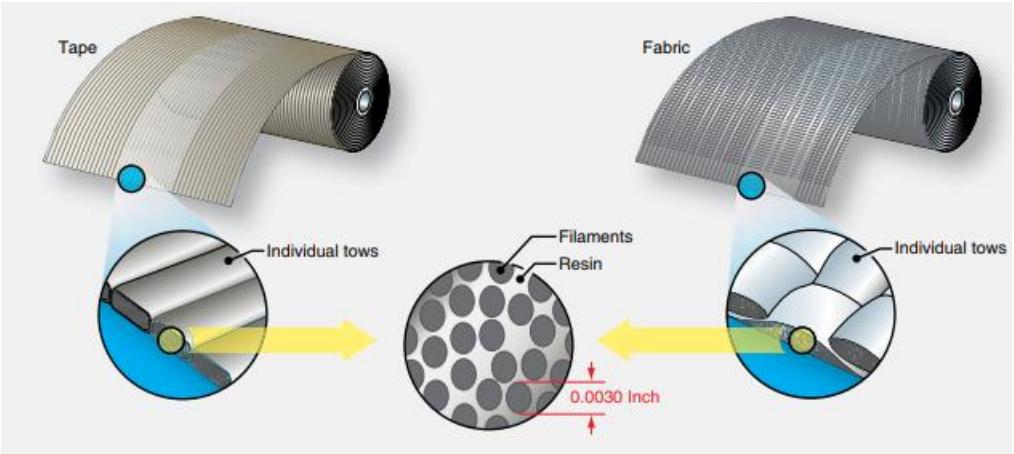

Figure 2.4 - Comparison between tape and fabric products [8].

2.2.2 Fibers

The most known fibers in industry are Glass, Aramid or Kevlar (very light), carbon (high modulus or high strength), boron (high modulus or high strength) and silicon carbide (high temperature resistant) but there are also the natural fibers such as cotton fibers and hemp fibers.

Fiberglass is nowadays widely used on leading edges of aircrafts, especially on areas on which underneath there are antennas or other communication systems installed, considering its easiness to conduct radio signals and for not conducting electricity contrary to metals. The most known types of fiber glass are the E-glass, also known as electrical glass due to its resistance to current transportation, and S-glass more often used on structural applications such as aircraft random and fairings due to its higher strength then E-glass [7,8].

Aramid fibers, also known as Kevlar®, are lightweight fibers with hight stiffness, hight resistance to impact and fire resistant, used on bullet-proof vests and also on aerospace industries such as aircraft engines cowling.

Carbon or graphite are also both similar fibers also widely used on industry due to its hight stiffness, strength and corrosion resistance. Carbon is widely used on structures that need to be strong and holding huge tensions.

Boron fibers are also known to have a great stiffness and strength however the filaments have a much higher diameter compared with the other common fibers which represents a limitation for its applications due to complex manufacturing process [1,2,8].

2.2.3 Matrix

In order to make a fiber made material to be used on a particular application and form, a matrix is required to bond the fibers and get a final composite material. The most common matrix materials are polymeric matrix such as thermoplastic resins or thermoset resins, among these the more known are the epoxy resins and polyimide resins. Mineral matrix such as silicon carbide or carbon is also widely used, especially for high temperature environments. There is also metallic matrix, normally metal alloys such as aluminium alloys and titanium alloys [2].

To understand how fibers and matrix behave independently compared with a composite material, figure 2.5 shows the stress-strain curve of these materials under a unidirectional tensile loads oriented. It can be observed that the fiber failure stress and also the stiffness is much higher than the matrix. On the other hand, matrix has a higher ductility and strain at failure than the fiber. The combination of these two materials into a fiber reinforced material results in a composite material that shows a failure strength and failure strain values in between of the values occurred with those materials separated.

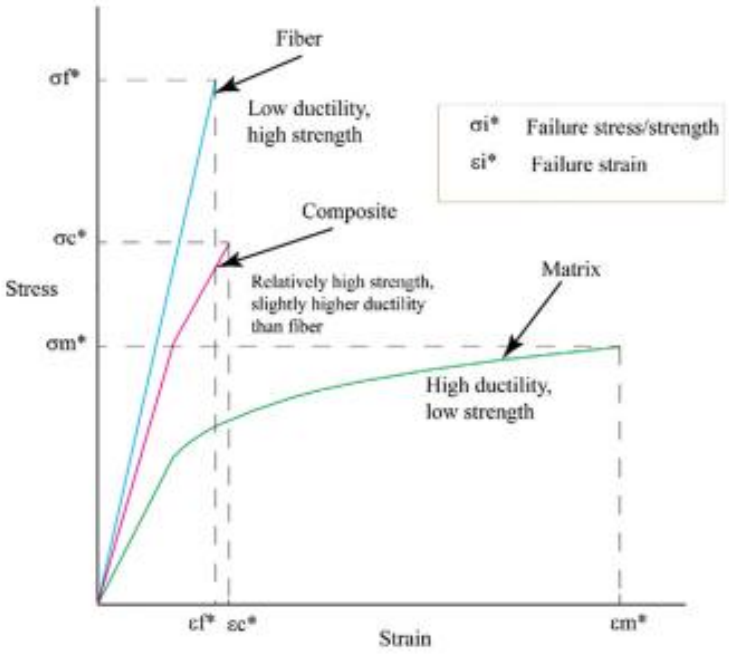

Figure 2.5 - Stress-strain curves of reinforced fiber composite material and comparison with respective fiber and matrix separated [2].

Normally, the component of a composite material that takes most mechanical loads are the fibers [4]. Fibers exhibit great strength and stiffness properties, as can be observed in table 2.1. Those fibers can be compared with structural materials such as Aluminium and steel also listed in table 2.1, and it can be seen that fiber properties are similar or some even better than the metals [5].

Table 2.1 - Common Fiber Properties [1].

Fiber or Wire	Density, ρ lb/in^3 (kN/m^3)	Tensile Strength, S 10^3 lb/in^2 (GN/m^2)	S/ρ 10^5 in (km)	Tensile Stiffness, E 10^6 lb/in^2 (GN/m^2)	E/ρ 10^7 in (Mm)
Aluminum	.097 (26.3)	90 (.62)	9 (24)	10.6 (73)	11 (2.8)
Titanium	.170 (46.1)	280 (1.9)	16 (41)	16.7 (115)	10 (2.5)
Steel	.282 (76.6)	600 (4.1)	21 (54)	30 (207)	11 (2.7)
E-Glass	.092 (25.0)	500 (3.4)	54 (136)	10.5 (72)	11 (2.9)
S-Glass	.090 (24.4)	700 (4.8)	78 (197)	12.5 (86)	14 (3.5)
Carbon	.051 (13.8)	250 (1.7)	49 (123)	27 (190)	53 (14)
Beryllium	.067 (18.2)	250 (1.7)	37 (93)	44 (300)	66 (16)
Boron	.093 (25.2)	500 (3.4)	54 (137)	60 (400)	65 (16)
Graphite	.051 (13.8)	250 (1.7)	49 (123)	37 (250)	72 (18)

The Average S/ρ and E/ρ, strength-to-density ratio and stiffness-to-density ratio respectively, are listed on table 2.1 considering that those are common indicators for material selection, especially for weight-sensitive applications. It can be concluded that by comparison with typical structural materials listed (aluminium, titanium and steel), fibers shown a higher strength-to-density and stiffness-to-density, however it should be noted that fibers require a matrix do get the final reinforced material, which is not required by common structural materials [1].

2.2.4 Laminated Composite Materials

As mentioned, the final properties (like strength and stiffness) of a composite material made with fibers depend on the orientation of the fiber layers, as it can be unidirectional, bidirectional or quasi-isotropic layup [6,7]. The quasi-isotropic composite materials are built with typically 0º, -45º,45º and 90º sequence, as illustrated in figure 2.6. This orientation buildup aims to perform like a isotropic material. This last solution is one of the most used types of composites used in aerospace industry, essentially made of fiber glass, carbon fiber and Kevlar [8].

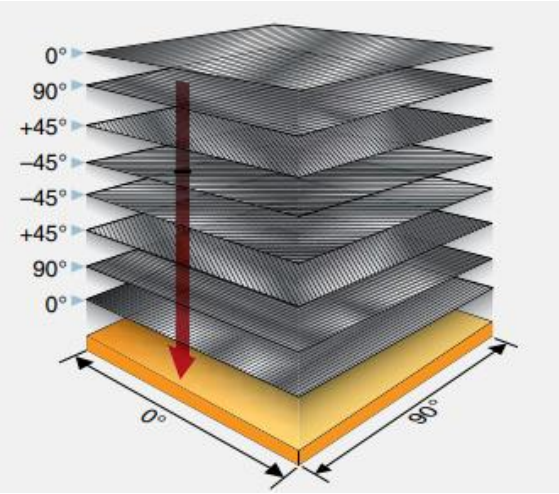

Figure 2.6 - Quasi-isotropic composite material layup [8].

Laminated composite materials are made of at least two different materials bonded together in layers. One of the best-known examples is the laminated windshield, which uses alternating layers of glass and plastic to achieve its protective behaviour. The plastic layer increases the stiffness and energy-absorbing capacity of the glass, providing far greater resistance to impact than an ordinary single-pane window. In addition, this layered structure helps prevent shattering, keeping broken pieces adhered to the plastic layer for enhanced safety. As a result, laminated composites are widely used in applications where strength, durability, and safety are essential.

Laminated composite materials can also be classified as laminated fiber-reinforced composite material which basically uses fiber composite materials on its layers building creating a material with different strengths and stiffnesses in different directions [1]

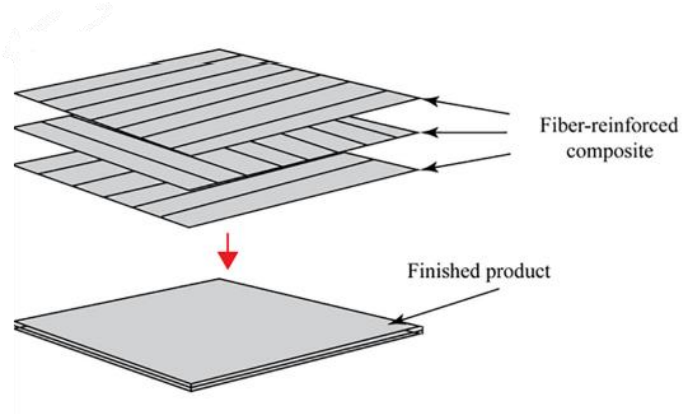

Figure 2.7 - Laminate composite scheme [2].

To have a perception on how currently the composites are replacing traditional structural materials, table 2.2 below presents several different fibers, and applications on aerospace industry:

Table 2.2 - Commonly used fibers in aerospace industry [4].

Fiber	Density (g/cc)	Modulus (GPa)	Strength (GPa)	Application areas
Glass				
E-glass	2.55	65 – 75	2.2 – 2.6	Small passenger a/c parts, air-craft interiors, secondary parts, Radomes, rocket motor casting.
S-glass	2.47	85 – 95	4.4 – 4.8	Highly loaded parts in small passenger a/c
Aramid				
Low modulus	1.44	80 – 85	2.7 – 2.8	Fairings: Non load bearing parts.
Intermediate modulus	1.44	120- 128	2.7 - 2.8	Radomes, some structural parts,rocket motor castings.
High modulus	1.48	160 - 170	2.3 – 2.4	Highly loaded parts.
Carbon				
Standard modulus (high strength)	1.77-1.80	220-240	3.0-3.5	Widely used for almost all types of parts in a/c, satellites, antenna dishes, missiles, etc.
Intermediate modulus	1.77-1.81	270-300	5.4-5.7	
High modulus	1.77-1.80	390-450	2.8-3.0 4.0-4.5	Primary structural parts in high performance fighters. Space structures, control surfaces in a/c
Ultra-high strength	1.80-1.82	290-310	7.0-7.5	Primary structural parts in high performance fighters, spacecraft.

In the last decade, one of the industries in which composite materials have played a key role on its development is the aerospace industry. The replacement of steel and aluminium by composite materials on commercial aircrafts, represented a huge efficiency improvement due to the reduction of weight, thus representing a significant decrease of fuel consumption [5]. Figure 2.8 below shows the utilization of composite material on the new generation aircraft Boeing 787.

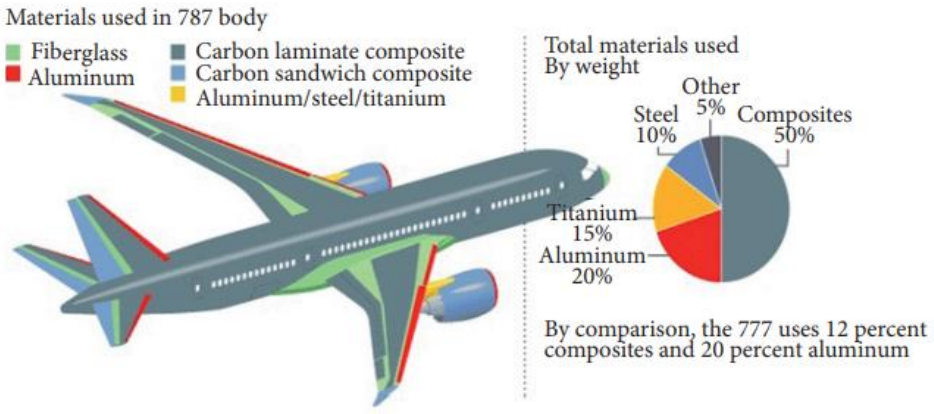

Figure 2.8 - Different material distribution on a Boeing 787 Aircraft structure [5].

2.3 Sandwich composite structures

The classification of sandwich for this kind of solution is self-explanatory as it basically uses a thick core material in between two external thinner face sheets of a different

material. These face sheets are bonded to the core using an adhesive layer, which serves as a bonding agent in order to create a strong interface between the different materials and the integrity of the entire assembly. Figure 2.9 below shows the scheme of a typical sandwich solution, which in this case uses honeycomb as a core material as two face sheets of aluminium, bonded with an epoxy resin as adhesive.

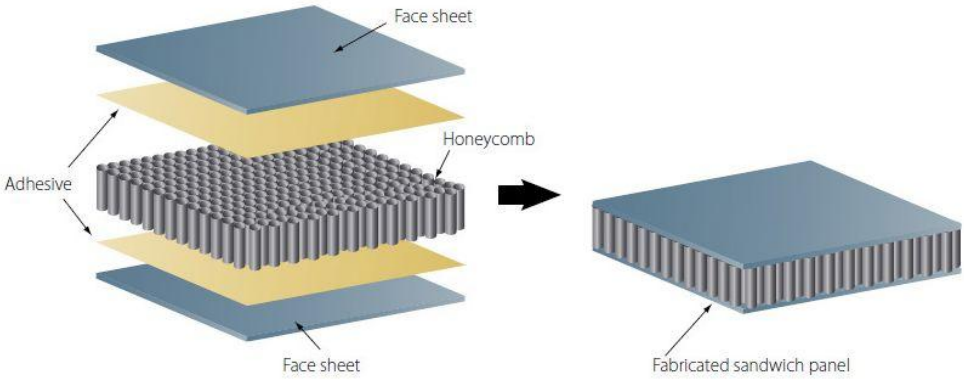

Figure 2.9 - Honeycomb Sandwich panel [9].

Sandwich structures are getting more and more usage nowadays as it delivers a satisfactory strength and stiffness behaviour which allows it to be an alternative to heavier materials such as structural metals. The reason for that is because when a sandwich structure is under flexural stress, meaning when the sandwich structure is being bended, the highest normal tension occurs on its external facings which are under tensile and compression loads so that the core could be of a low-density light weight material. The flexural strength of a rectangular cross-sectional beam is proportional to the cube of the thickness, so that by adding a core in between the face sheets it increases the thickness which then increases the flexural strength. The core of a sandwich composite material is also responsible to sustain the highest shear stress that occurs on a sandwich beam, so the core material should be shear stress resistant [10].

This kind of composite structure gives the enormous advantage of varying its geometry and materials to get outstanding properties for a wide different needs, reducing significantly its weight when comparing to a classic thick metal material. Figure 2.10 below shows that the increase of a sandwich composite stiffness is proportional to its core thickness which then considering the low density of its core material, it results on an extremely high stiffness/weight ratio [9].

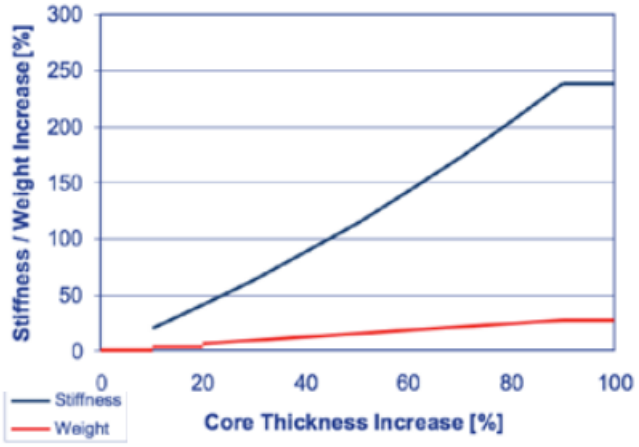

Figure 2.10 - Stiffness/weight with thickness increase of a typical composite sandwich material [6].

As presented on figure 2.10, this principle of increasing the thickness of the beam to obtain higher strength and stiffness is the same principle used on by typical “I” profile beams. As illustrated in figure 2.11 below, the I-beam also uses a long but thin web in between its face sheets in order to increase the beam thickness, remaining as lighter as possible, which in the case of the sandwich composite beams its represented by the core.

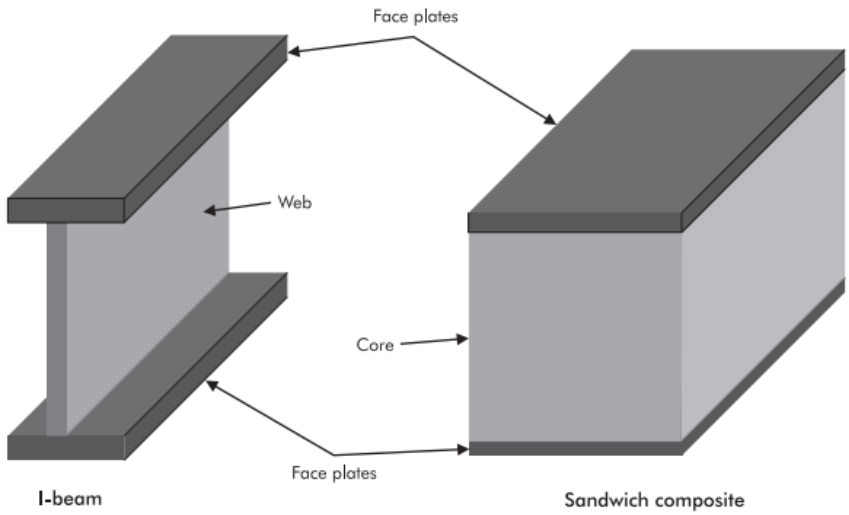

Figure 2.11 - Comparison between I-beam and sandwich composite beam [11].

2.3.1 Core Material

The core material should be selected considering its detailed advantages and disadvantages pending on the desired application. Table 2.3 presents the more common core materials used on sandwich composite structures the associated characteristics and benefits. On top of these characteristics, it is also important to understand the

material structural behaviour in different directions. The x-and y- direction loads will represent a potential failure due to buckling and shear effect, so the core selection must be done considering the capacity to withstand such loads. For specific core materials, the orientation its important due to the nature of the material for example balsa wood must be oriented in the z direction because the wood fibers natural orientation is in z-direction.

Table 2.3- Common core materials and their properties [11].

Core Material	Characteristics and Benefits
Balsa wood (end grain)	Good shear strength, high fatigue endurance, low cost, easily bonded, easily finished, good temperature range
Polyvinyl chloride (PVC) foam (crosslinked)	High strength, high stiffness, low cost, easily bonded
PVC foam (linear)	Low cost, easily bonded, good impact resistance
Polymethacrylimide (PMI) foam	High dimensional stability under heat, excellent mechanical properties, solvent resistance, low thermal conductivity, high strength and stiffness
Polyetherimide (PEI) foam	Low water absorption, high thermal stability, high strength, fire resistant, good dielectric properties
Styrene-acrylonitrile copolymer (SAN) foam	No outgassing, high stiffness, high impact and fatigue strength, no environmental problems with resin or recycling
Ceramic foams	Unsurpassed thermal resistance, excellent thermal insulation, solvent resistance
Paper honeycomb	Low cost, easily bonded, strong for weight
Polyimide paper honeycomb	High strength to weight, corrosion resistant, good thermal insulation, fire resistant, easily shaped, excellent dielectric properties, easily bonded
Polyolefin honeycomb	Rigid and elastic, high toughness, sound and vibration dampening, explosion containment vessels, scrim cloth available, high strength to weight, corrosion resistant, fungi resistant, can be thermoformed, recyclable
Engineering plastic honeycomb	Tough, relatively high-temperature tolerant, excellent dielectric properties, good thermal insulator, fire resistant, fungi resistant, highly variable cell sizes and densities
High-performance honeycomb	Carbon fiber reinforced, carbon-carbon, aramid, quartz, superior strength, superior thermal resistance
Metal honeycomb	Aluminum, titanium, stainless, nickel available, no outgassing, high-temperature tolerant, fire resistant, fungi resistant, high thermal conductivity
Stitched/compressed	Excellent drape, needs to be fully wetted, high impact resistance, reduces cracks, absorbs resin for added strength

2.3.2 Facings

Facings, face sheets or skins are common terms used for the upper and lower material sandwiching a core. The skin material is relatively thin when compared to the core. Skin materials are normally made of materials with great tensile strength such as metals like aluminium or composite materials like Kevlar®, fiberglass or carbon fiber. The facing is

composed by plies of fibers, oriented in particular directions as mentioned. The plies of fibers are bonded by a matrix which together represents a reinforced composite material, which represents the x-y plane stiffness and strength of the sandwich, by increasing the amount of fiber plies and orienting those in the direction of the forces, the sandwich capability to sustain x-y plane loads will increase.

2.3.3 Matrix

As mentioned during the composite materials state of the art review, matrix is the material responsible to connect the different materials, either to link the facings to the sandwich structure core or to glue the different plies of fiber to build a layer of reinforced fiber. The matrix to be used on its different applications and constructions should be selected considering its chemical stability against the other materials used and also the best mechanical properties. When a matrix bonds two layers of the same material and it results on the migration of molecules from the matrix to the inherent materials and the other way around, it is considered a chemical matrix joining. On sandwich structures, the most commonly used matrix are the adhesives, which normally suffers chemical and physical changes to went from liquid phase to hardening phase [11]. The most commonly used adhesives are the cured polyurethanes, however epoxy resins are also widely used, and for cork sandwich structures it has proved to perform better than any other [11].

2.4 Cork

Cork is the material that grows around the oak tree as skin layer, as shown by figure 2.12. It is botanical called as the periderm layer that grows naturally on the skin of the tree due to phenomenon of phellogen, also known as cork cambium [12]. This phenomenon is basically a cell generation process that enables the accumulation of cells, turning into a thicker layer. This process is especially important because allows its continuing formation even after the removal of the complete layer of skin from the tree, making cork a renewable material [13].

Figure 2.12 - Cork section cut in the tree [14].

The most known oak tree species that produces cork, has the scientific name of *Quercus suber L.* and it can only be found on the Western Mediterranean area [12]. It is largely produced by Portugal and Spain, but it can also be found in southern France, Italy and in North African Countries as can be seen on the figure 2.13. *Quercus suber L.* is not the only species of tree in the world that produces cork, there is also *Betula Pendula*, *pinus Pinaster, Pseudotsuga Menziessi, Quercus Cerris* and others [14]. However, those provide cork with different properties which doesn't meet the quality of *Quercus suber L*.

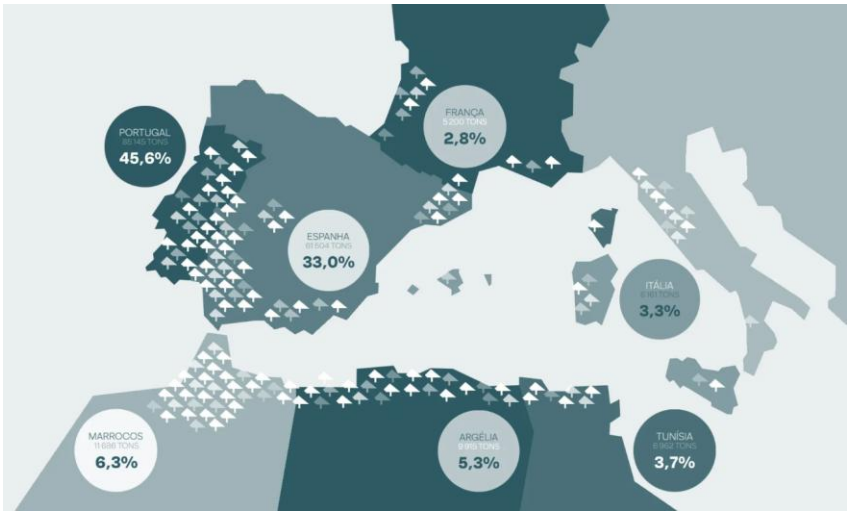

Figure 2.13 – Production of cork per country [15].

2.4.1 Cork Harvesting

There are some minimum conditions that need to be verified on each oak tree, to consider it ready to be harvested for the first time. The tree needs to have a minimum of 0,70 meters of perimeter on its trunk, and 1,30 meters high from the ground [13].

Then the cork removal is a manual and meticulous process that is done by individual personnel using an axe as a tool. This process consists of doing long linear cuts in vertical position against the tree trunk and branches where the cork is, to obtain long and large planks of cork as can be seen in figure 2.14. This process requires high precision to avoid damaging the inner skin of the tree, which can cause the loss of cork growth capability of the tree [16]. Then, after removing all the cork from the tree, the trunk is marked with a number of the year when it was removed, and it starts the counting of another minimum 9 years until the next harvesting.

Figure 2.14 - Cork being removed from the oak tree [15].

The removal process takes place between May and August, pending on the climate during this period as it requires long periods of warm temperatures and low humidity conditions before the removal [17].

The first Cork harvesting of the oak tree provides cork categorized as “virgin cork”, which shows an irregular outer surface and density. It is normally used to be industrial processed to produce agglomerates [17]. The more aging of the tree, the better quality of the cork it provides. On average, it is only after the third harvesting, that an oak tree is capable to provide cork good enough to be used as bottle tops, the famous so-called cork stoppers. At this stage, the cork is called “reproduction cork”, which will grow from the tree for the next two hundred years on average, which provides around 15 harvests of this high-quality cork [13].

After the harvesting, cork planks are mounted in a typical huge stack (figure 2.15), which normally contains the total amount of cork supplied by the oak trees that were harvested on the same period on the same area and will then rest there for at least 6 months to stabilize exposed to the local climate conditions such as sun, air and possibly rain. After this period, cork can then be evaluated, most of the cases sold to follow its industrial destination [15].

Figure 2.15 - Stack of cork after harvesting [15].

2.4.2 Macroscopic Analyses

After the cork harvesting, a new cycle of cork growth starts by the getting new accumulated cells on the skin of the trunk which will turn it a new cork exterior layer, called cork back, then subsequent layers of cells will accumulate until it turns a thick cork plank, after around another 9 years [13]. The inner cork (interior skin of cork plank) is the last layer of cork produced by the tree before its harvesting, it's also called as "belly" and shows less flexibility when compared with the other layers of the material. The macroscopic analysis is very important as some characteristics are directly related to the quality of the material.

The observation of lenticular channels along the side section of a cork sample as can be seen on figure 2.16, its size and density are strictly related to the porosity of the cork which is a key factor to determine its quality. Also, other macroscopic observations such as smoothness, colour and size of the cork back are related to its quality [13,17]

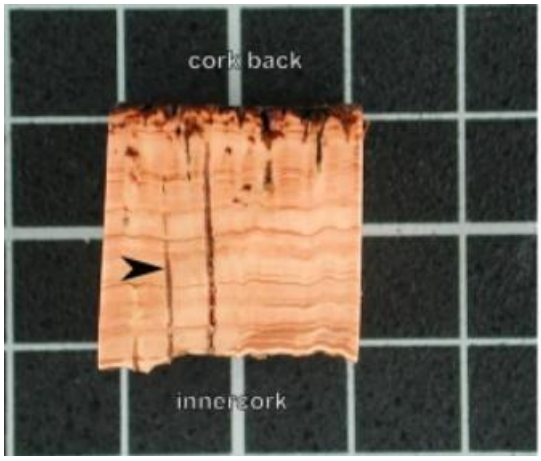

Figure 2.16 - Section cut of a cork sample [19].

2.4.3 Microscopic Analysis

The microscopic observation of cork was done by the first time by Robert Hook in 1665 [12]. Later, after several studies specially by Natividade in 1938 and 1950, it was reinforced the conclusion that cork is a homogeneous tissue made of cells that have lost their content during its growth but filled with air, which are arranged with no empty space nor communication between them [13]. Cork cells have a rectangular prism geometry and are organized in parallel layers in radial direction and similar to a brick wall in tangential direction [19], an illustration can be seen in figure 2.17.

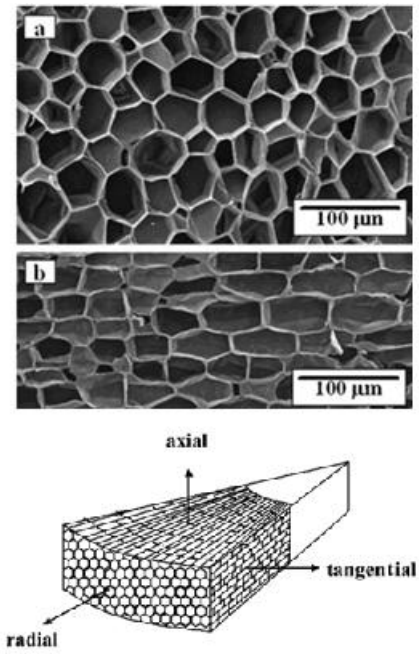

Figure 2.17 - Cork cellular disposition in cork: a) radial section and b) tangential section [12].

Another important observation is the thickness of the cork cells. Considering that the cell wall is roughly constant as shown in figure 2.18, the total density of the material depends on the thickness and dimensions of the cell walls and its corrugations within a ring of

grown material [12]. The cell walls deliver key properties to cork such as isolation and toughness. Specially, the Secondary cell wall which mainly contains suberin and lignin polymers, that provides an insolation layer making it waterproof. Also, the other walls such as tertiary and medium lamella are made up with cellulose lignin which delivers toughness to the cells [12,17,20].

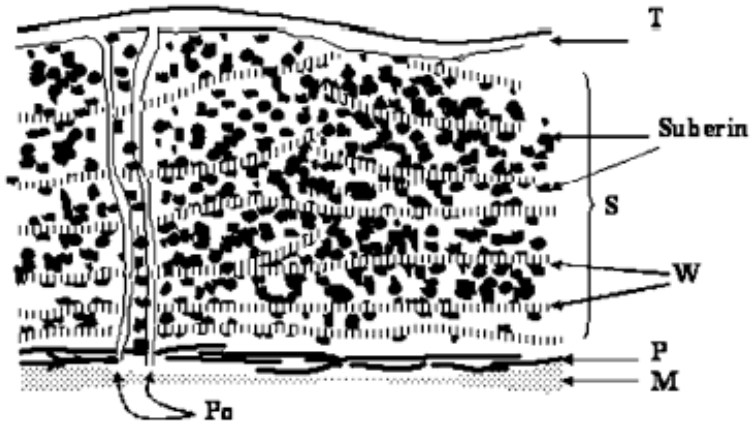

Figure 2.18 - Cork Cell wall scheme: (T) tertiary wall, (S) Secondary wall, (W) Waxes or polymers and suberin, (P) Primary wall, (M)Medium lamella, (Po) Pore [12].

2.4.4 Mechanical Analyses

The nominal stress-strain curve of cork in compression as presented on figure 2.19, shows a first area that corresponds around 10% of strain and is related to the elastic compression of cell walls, then a horizontal continuity up to 60% of strain which corresponds to a continuous buckling of the cell walls and then, the third area corresponding to the almost complete displacement of material area from its initial shape due to its high compression [21].

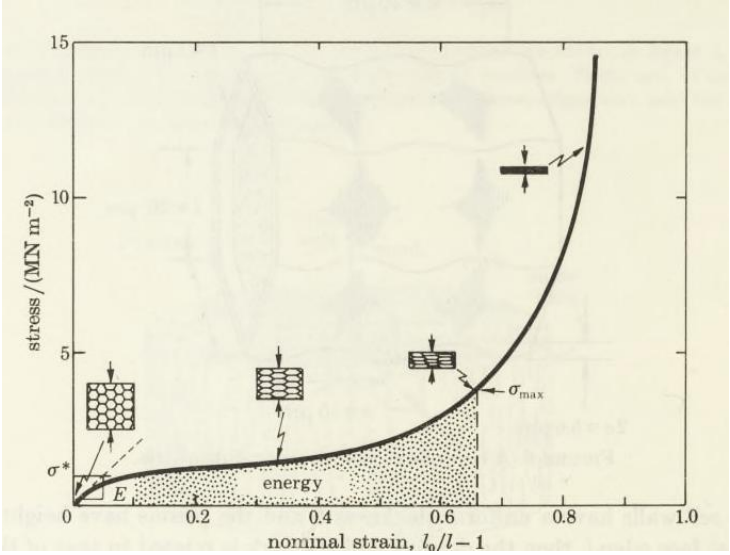

Figure 2.19 - Nominal Stress-Strain Curve of cork in compression [21].

Moreira *et al* [22], performed a quasi-static compressive test in 8 specimens obtained from the same cork plank and observed a compressive behaviour typical of a homogeneous isotropic material, with a result of a 7.4 MPa *Young's* modulus. Different speed tests were made using several specimens (C3 specimens at 5 mm/min, C6 specimens at 10 mm/min and C8 specimens at 20 mm/min), whose results are shown in figure 2.20. It can be observed that by the coincidence of the different curves, cork is not sensible to the strain rate.

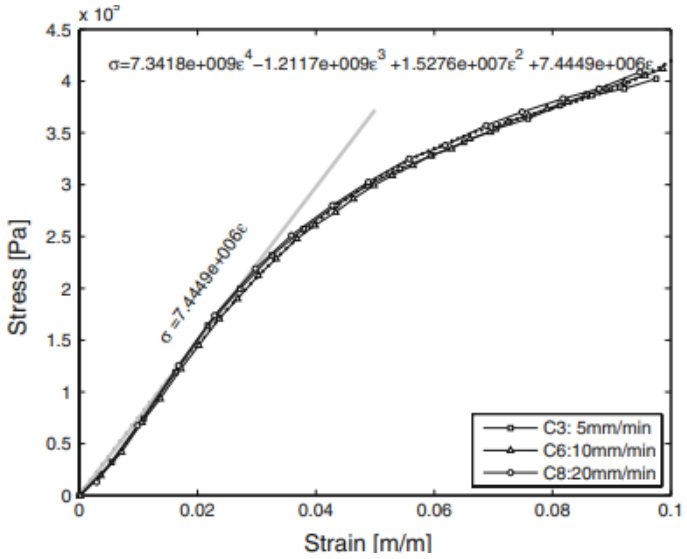

Figure 2.20 - stress-strain curve of cork obtained on a quasi-static compressive test on specimens C3, C6 and C8 [22].

Using the same equipment and testing conditions as applied in the compressive test, five specimens were subjected to tensile tests at a test velocity of 5,10 and 20 mm/min. The results obtained, which were satisfactorily correlated, evidenced an initial mean elastic modulus of about 17.4 MPa as per figure 2.21 (standard deviation: 1.3 MPa), which is clearly higher than the modulus obtained from the compressive test. This observation is in accordance to the information provided by several researchers [8,24-26] and, as described before, can be explained by the initial corrugation of the cell wall, which causes the cell walls to interlace, representing a dragging effect between cell walls, increasing the tensile strength.

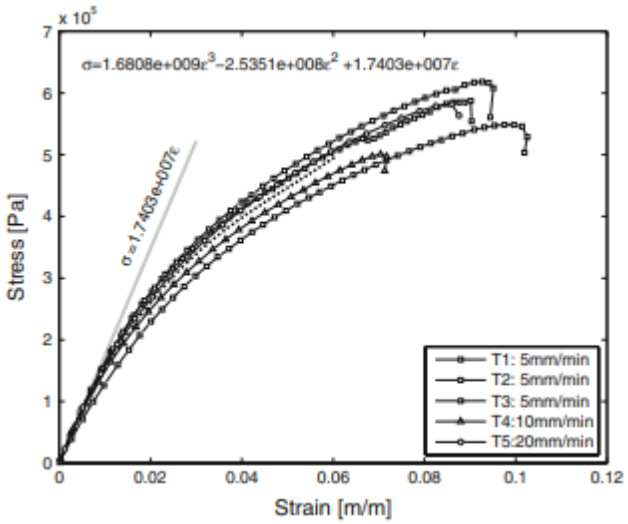

Figure 2.21 - Tensile load-displacement curve of cork [22].

Also, Massimiliano *et al* [23], performed similar tests on several samples of raw cork and obtained similar results. Both studies highlight the strong stiffness of the material and good compressive behaviour.

Cork is also characterised by its low thermal conductivity due to the presence of air inside the cells, which represents a great solution for thermal isolation but also for sound isolation.

Following the purpose of this study, it is very important to compare cork with other materials used in most usual composite solutions. As it is an organic material it is hard to compete with synthetic materials, as can be seen on figure 2.22 below.

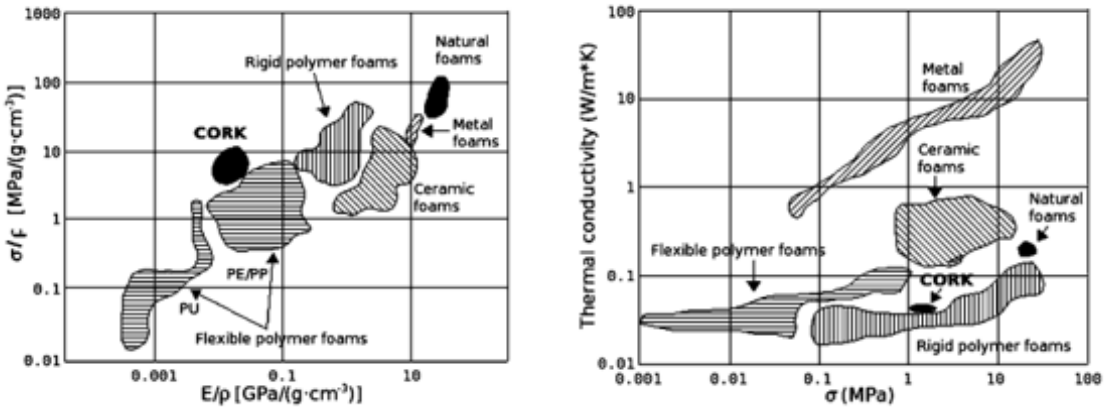

Figure 2.22 - Comparison of Cork and other materials [23].

As shown the best materials are on the top right corner and there are some foams with higher capability to resist to mechanical loads then cork, however cork presents a good compressive strength, and a low thermal conductivity as mentioned before so for such applications it will be a great solution as we can see on the right hand-side graph.

2.5 Sandwich Beam Experimental Analysis

A sandwich structure can be subject to tensile, compressive and shear stress as illustrated in figure 2.23. The design criteria should be in accordance with its application and the same applies for the tests that should be performed. Shear is the most common design criteria in sandwich structures construction as it can affect the materials in different ways and directions. The majority of sandwich beams and panels are subject to compressive and bending loads. The core material is mostly affected by shear stress while the facings are under compressive and tensile stress. Considering that, a research was done on the experimental tests performed on similar sandwich constructions and more exactly with a core made of cork. It was concluded that the most common tests are the three-point bending and four point-bending flexural tests.

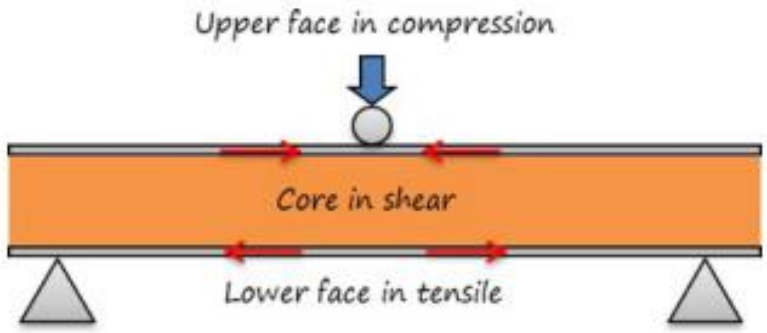

Figure 2.23 - Sandwich structure 3PB stresses [6].

By bending the sandwich beam, the core shear strength, tensile and compressive strength are tested and also, it allows to get enough data to build the load-displacement or stress-strain curves of the specimen, which then can be used to compare different sandwich constructions with different materials, and to allow the design of each construction to be improved.

As mentioned, a literature review was conducted to understand what has been done so far with regards to experimental testing of sandwich structures and some interesting and relevant cases for these studies are summarized below:

João Lopes *et al*. [24], performed a three-point bending tests on several sandwich structures, all with a carbon fiber-epoxy fabric 0º/90º laminate faces using different cores of cork agglomerate, Honeycomb and Rohacell foam. They verified that on the honeycomb and Rohacell core made sandwich specimens, the failure modes were crushing of the face in compression, and core collapse. On the cork core made sandwich specimens, they obtained also the face crushing but with the core having longitudinal cracks in the direction of the specimen's extremity. They concluded that the fracture of cork core is intergranular, pointing that the weakness of the cork agglomerate cores is its matrix.

Silva *et al*. [25] performed 3-point bending tests in accordance with ASTM C393-00 on several specimens made with agglomerate cork core material (combination of cork and resin) and a top faces-sheet made of 3 layers of carbon fiber build in 0º/45º/0º. When compared with typical PMI (Polymethacrylimide) and honeycomb sandwich composite specimens, concluded that the cork made specimens had a difference of less 1% to 12% less resistance to shear stress but an increase of 38 to 56% more resistance then the PMI composite solution. It can be seen on figure 2.24 that specimens of cork cored sandwich shown a smooth core failure with crack propagation as pointed by number 2 to point 3 of the load-displacement curve, showing the ductile behaviour of cork on its longitudinal direction as a failure mode and on figure 2.25 (specimens with PMI and honeycomb core), the failure mode was the compression facing failure by fracture which can be seen on the point 2 of the load-displacement curve.

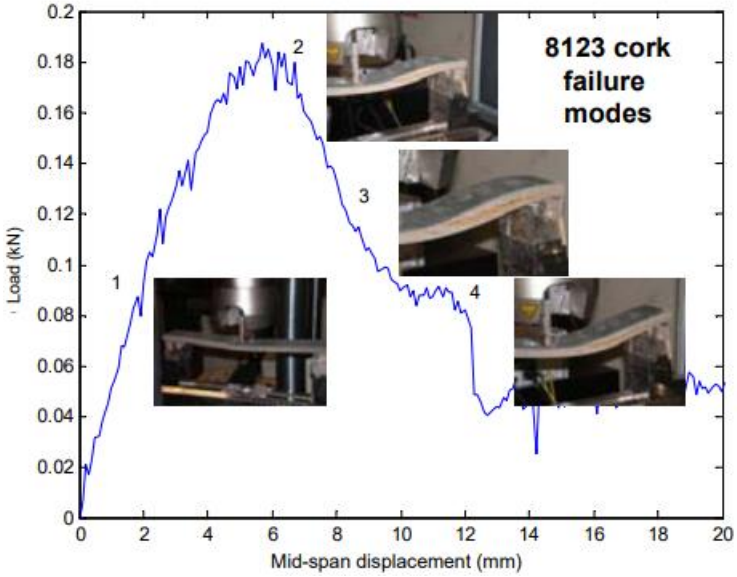

Figure 2.24 - Load-Displacement curve of cork core made sandwich specimens [25].

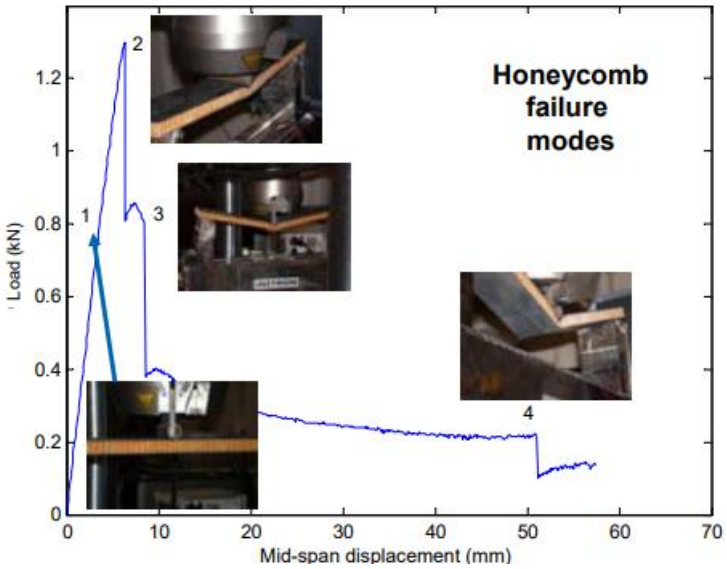

Figure 2.25 - Load-Displacement curve of honeycomb core made sandwich specimens [25].

Daniel, Isaac & Gdoutos [26], developed a failure mode study of several sandwich beam specimens, manufactured with a 8-ply unidirectional carbon/epoxy (AS4/3501-6) facings and 2 different sets of PVC foam Divinycell H100 and H250 as a core, under a three and four-point bending tests and verified that facing wrinkling failures were observed on both three- and four-point bending tests but core failure occurred only under a three-point test, concluding its failure by shear stress. Although this study didn't use cork, it is relevant to understand how the 3PB and 4PB tests were performed on other composite sandwiches.
Ivo Rosário [27],developed a viability study of the cork usage as a core composite material instead of a typical PMI foamed core material on sandwich panels, used generally on secondary structure of aircrafts, and concluded that cork sandwich panels performed better as result of its light weight, but also with the advantage of a recycle possibility after the replacement of such panels which is frequent during the lifetime of the aircrafts.

2.6 Numerical Analysis of Sandwich Beams

In order to test, validate or identify potential failures, a numerical analysis can be performed using the Finite element method (FEM), which can be done by providing to a software the geometry, materials properties and calculation settings. There are several software options for this kind of approach, but the most utilized ones on similar research studies and design projects are *Ansys* and *Abaqus*. The literature research, presented several studies with similar objectives, aiming to validate the experimental results with a numerical analysis.
Using *Straus7* finite element program, Selvarayan et al [28] carried out a four-point bending test simulation on a sandwich specimen made of carbon fiber skins and a core made of agglomerated cork and concluded that the numerical solution showed a good correlation with the experimental results within the linear elastic domain, however, they observed a bad correlation from experimental results beyond the elastic regime.
Demis Peixoto [29], performed a numerical analysis on sandwich specimens made of carbon fiber facings and a core of honeycomb shaped agglomerated cork, simulating with software *Abaqus* the 3PB experimental test in accordance with ASTM/393/C393M-11. The author compared the elastic regime of the experimental data with numerical data and concluded that the FEM was within the various experimental results obtained from different specimens tested. He highlighted that values immediately after elastic regime had a different trend then the experimental regime.
B Muralidharan [30], presented a numerical analysis of a Sandwich specimens made of Carbon fiber facings and a core made of PLA, on which several simulations were performed on a 3D model of the specimen using *Ansys Workbench.* The 3D simulations

presented a core failure, similar to experimental results. However, the displacement values were significantly different when compared to the experimental results.

2.7 Sandwich Beam Failure Modes

The sandwich structures are mostly used to cover other structures and provide its contour, such as aircraft wing structures aircraft body fairings, being subject to compressing force and shear effect.

On this study, three sets of sandwich beam specimens were tested under a three-point bending tests, which calls for several common failure modes such as compression and tensions failure of its skin faces, debonding of the faces to core connection, buckling and core collapse [26]. A lot of research has been made on those failure modes. Wrinkling of the sandwich beams facings under compression and bending effect was investigated by Thomsen [31]. Compression failure of sandwich beams facing in uniaxial stress by fracture was studied by Zenkert [32]. Core failure due to shear effect has been investigated by W.G Heath [33].

Such investigations allowed the understanding of the different properties interaction and its effect on the sandwich structures. Below, on figure 2.26, are illustrated the more common failure modes (a) for facing fracture, (b) for the core failure examples and (c) and (d) for local buckling also known as wrinkling.

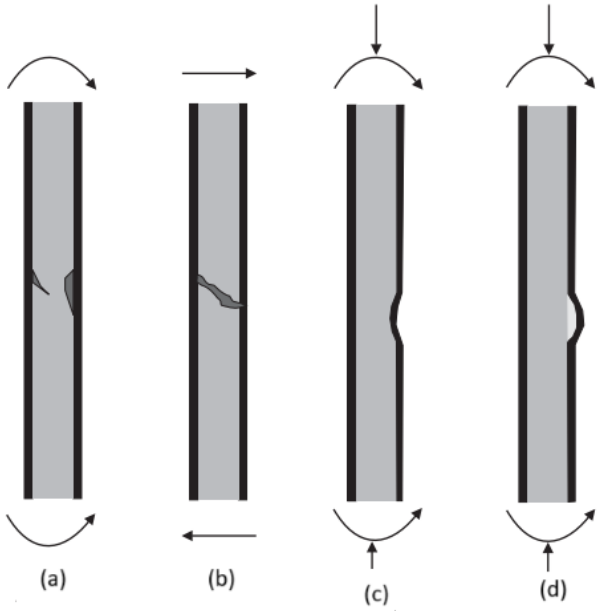

Figure 2.26 - Sandwich beams typical failure modes: (a) for facing fracture, (b) for the core failure examples and (c) and (d) for local buckling [11].

In order to understand the observed results and failure modes of the experimental testing, it's important to go into detail of those failure modes which are result from different types of load effects such as compression, bending and shear stress.

2.7.1 Facing yielding/fracture

Whether yielding or fracture as a failure criteria, the critical stress of the facing material before its failure is given by ASTM C393 [35] and presented below as follows:

$$\sigma = \frac{PmaxL}{2t(d+c)b} \tag{2.1}$$

Where:

σ = facing bending stress (MPa)

$Pmax$ = maximum load (N)

d = sandwich thickness (mm)

c = core thickness (mm)

b = sandwich width (mm)

L = span length (mm)

t = facing thickness (mm)

2.7.2 Facing Wrinkling or local buckling

The wrinkling effect occurs when the compressive stress on the sandwich beam is higher on its compression facing then the shear stress. Wrinkling can be characterized as a small buckling on the compression facing as shown on figure 2.27. When shear stress is higher than the compressive stress of the facing, the crushing of facing surface will occur primary to wrinkling, however it is common to obtain face crushing around the load contact zone immediately after wrinkling [11,19,29].

The elementary approach to the wrinkling failure mode is the Winkler foundation problem, which considers that the core material doesn't experience a shear stiffness ($G_{cxz} = 0$) when facing wrinkling occurs. And so, a critical facing wrinkling stress (σ_{cr}) is given by:

$$\sigma_{cr} = \sqrt{\frac{2}{3}\frac{h_f}{h_c}\frac{E_c E_f}{(1 - v_{xy}v_{yx})}} \tag{2.2}$$

Where:

h_f, h_c are the compressing facing and core thickness, respectively

E_c E_f are the core and compressing facing elastic modulus, respectively

v_{xy}, v_{yx} is the Poisson's Ration of the facing in longitudinal and transversal direction respectively.

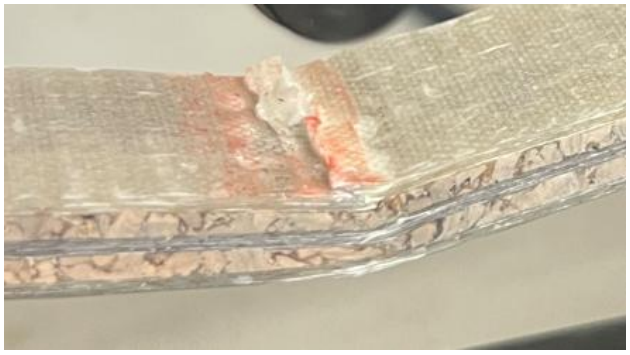

Figure 2.27 – T3 Specimen Face Wrinkling

Hoff et al [34] on the other hand, presented an approach addressing the shear stress in the core, considering that tensile and compressive stresses in the core perpendicular to the face occur due to face wrinkling, so that core shear modulus (G_c) had to be accounted as follows:

$$\sigma_{cr} = 0.5\sqrt[3]{E_f E_c G_c} \tag{2.3}$$

Where:

E_f= Facing elastic modulus

E_c= Core elastic modulus

G_c= Core shear modulus

2.7.3 Core failure or fracture

Specifically on three-point bending tests, on which the shear stress is normally high enough, the core failure may occur considering that the core material is responsible to support most of the entire transverse force. The critical shear stress for core material on sandwich beams is given ASTM C393 [35] and presented by:

$$\sigma_{cshear} = \frac{G_c h_c}{2t_f} \quad (2.4)$$

Where:

t_f= face sheet thickness

G_c=core shear modulus

h_c=core thickness

3 Experimental Analysis

3.1 Sandwich Specimens Manufacturing

The first step for the sandwich composite manufacturing was to prepare the support base and the mold on which the materials were inserted to start building the sandwich. A wood mold and support base were manufactured with dimensions 400x400 mm, a bleeder was trimmed with the same size of the mold base, same for the peel-ply, fiber glass layers and agglomerate cork. Then a support base was prepared and applied a bleeder to accommodate the first laminated fiber glass composite and to absorb the epoxy resin overruns. A peel-ply was also positioned on top of it to enable a soft and easily mold removal after the finishing of the cure process. Next, the laminate reinforced composite was built by bonding the layers of fiber glass with bidirectional 0º/90º/0º stacking, brunching the epoxy resin under each layer and on top of the upper layer. A top cover was placed on top of the composite material, and it was dried at atmospheric pressure and 25ºC controlled temperature. This procedure was done to get a 2F (two fabric plies), 4F (four fabric plies) and a 5F (five fabric plies) laminate face-sheet which was used in different configurations to obtain 3 different types of specimens, as shown further ahead. Having the face-sheets manufactured, a cork agglomerate cork was placed in between the face-sheets and inserted into the mold, where it was placed into the wood made mold and compressed with a 50 kg weight in order to remove air bubbles between the layers

of material and provide proper bonding between layers of material and its adhesive which in this case was the same used for the matrix (epoxy resin).

Finally, it was time to remove the sandwich from the mold as shown in figure 3.1 and then to measure and trim it into several specimens to be tested.

Figure 3.1 - Experimental Sandwich Composite after mold removal.

The piece produced was then cut into sandwich specimens with 250x20 mm considering the procedures referred in 3.2 and presented below the profile of the three types of specimens obtained:

Figure 3.2 - T1 (5F/1C/5F) Sandwich Specimen.

Figure 3.3 - T2 (4F/1C/2F/1C/4F) Sandwich Specimen.

Figure 3.4 - T3 (5F/1C/5F/1C/5F) Sandwich Specimen.

Type 1 Specimens (T1), represented on figure 3.2, are made of 5 layers of fiberglass/1 layer of agglomerated cork/5 layers of fiberglass (5F/1C/5F), with a total thickness of 4.65 mm.

Type 2 Specimens (T2), represented on figure 3.3, are made of 4 layers of fiber glass/1 layer of agglomerated cork /2 layers of fiberglass/1 layer of agglomerated cork /4 layers of fiberglass (4F/1C/2F/1C/4F) with a total thickness of 6,4 mm.

Type 3 Specimens (T3), represented on figure 3.4, are made of 5 layers of fiberglass/1 layer of agglomerated cork/5 layers of fiberglass/1 layer of agglomerated cork /5 layers of fiberglass (5F/1C/5F/1C/5F) with a total thickness of 8mm.

Table 3.1 shows the dimensions of the different types of specimens used on this study.

Table 3.1 - Dimensions of the three types of Specimens.

Specimen	Composition	Layer thickness [mm]	Total thickness (d) [mm]	Width (b)[mm]	L=20x(d) [mm]
T1	5F	1.34	4.65	20	93
	1C	1.97			
	5F	1.34			
T2	4F	1.07	6.4	20	128
	1C	1.86			
	2F	0.53			
	1C	1.86			
	4F	1.07			
T3	5F	1.34	8	20	160
	1C	2			
	5F	1.34			
	1C	2			
	5F	1.34			

Having the first laminated fiber-glass composite built, measurements were performed to obtain its heigh, width and mass.

The fiber and matrix mass fractions are an important parameter to determine whether the fractions obtained are in line with the typical fractions that are expected to be verified when manufacturing a reinforced composite laminate material.

Fiber mass fraction is defined as:

$$Mf = \frac{Mass\ of\ fibers}{Total\ mass} \tag{3.1}$$

And so, matrix fraction is:

$$Mm = \frac{Mass\ of\ matrix}{Total\ mass} \tag{3.2}$$

With

$$Mm = 1 - Mf \tag{3.3}$$

The volume fraction is then defined as:

$$Vf = \frac{Volume\ of\ fibers}{Total\ volume} \tag{3.4}$$

$$Vm = \frac{Volume\ of\ matrix}{Total\ volume} \tag{3.5}$$

The Density of the ply can be obtained as follows:

$$\rho = \frac{Total\ mass}{Total\ volume} \tag{3.6}$$

Mass of fiber and Mass of Matrix and the total mass was obtained by weighing the dry fiber and dry matrix before the reinforcement and then weighing the reinforcement of the layer. Same procedure was made for volume measurement.

The number of grams of mass of fiber per m^2 Mf is given by the expression below, on which b is the ply thickness:

$$b = Total\ volume\ \times \frac{Mf}{fiber\ volume \times \rho_f} \tag{3.7}$$

Considering that multiple plies were stacked, b should be obtained dividing the total thickness of the layer by the number of plies. Measuring the layer thickness obtained after reinforcement process, the value of b was obtained [6].

From equation (3.7) above, the mass fraction was obtained and with the relations above from (3.1) to (3.5) and table 3.2 below shows the fiber and matrix fractions obtained on both 5F and 4F reinforced fiber/epoxy composite layers.

Table 3.2 - Reinforced fiber-glass mass and volume fractions.

Specimen	Nr of Reinforced Plies	Fiber-glass Mass fraction	Epoxy Mass fraction	Total Volume (m^3)
T1	10	57.36%	35.26%	3.93 E-003
T2	10	49.24%	38.75%	5.70 E-003
T3	15	54.37%	37.05%	6.73 E-003

3.2 Experimental Methodologies

The adopted experimental procedure consists of performing 3-point bending tests on three different configurations of handmade specimens of sandwich beams with a core of agglomerate cork and layers of epoxy/fiber glass. The tests were performed in accordance with the ASTM Standard Test Method for Flexural Properties of Sandwich Constructions, designation: C 393-00. The goal of this testing is to determine the sandwich beam flexural stiffness, the core shear strength and shear modulus considering that the sandwich stiffness and core shear modulus can be calculated using the deflections measured of the sandwich flexure specimens.

There are several parameters that should be considered to ensure that the simple sandwich beam theory is valid during these tests is to make sure that the span length divided by the sandwich thickness should be greater than 20 (L/d>20) with the ratio of facing thickness to core thickness less than 0.1 (t/c <0.1) [35].

Also, the width should not be less than twice the total thickness, not less than three times the dimension of a core thickness, nor greater than one half the span length. The specimen length shall be equal to the span length plus 50 mm (2 in.) or plus one half the sandwich thickness whichever is the greater [35].

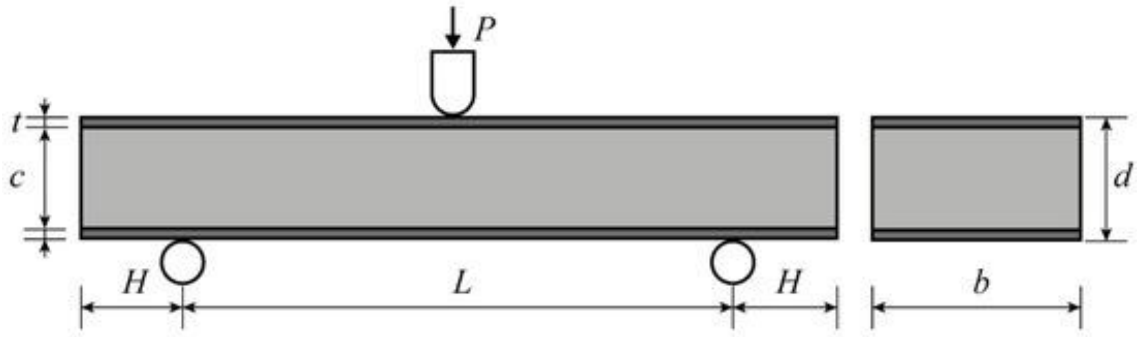

Figure 3.5- Three-point bending test specimen sketch [25].

3.2.1 Verification of conformity with ASTM Standard Test C 393-00

"The span length divided by the sandwich thickness should be greater than 20 (L/d>20) with the ration of facing thickness to core thickness less than 0.1 (t/c <0.1)."

- ✓ The Span length was calculated following this requirement as shown on table 3.1 so that T1, T2 and T3 specimens were tested with 128, 93 and 160 span lengths respectively.

"The ratio of facing thickness to core thickness should be less than 0,1 (t/c <0,1)."

- ✓ T1 specimens have a face thickness (t) of 1.2 mm and a core (c) of 2 mm, so t/c=0.6 which follow the norm.
- ✓ T2 specimens have a face thickness (t) of 1 mm and a core (c) of 4 mm, so t/c=0.25 which follow the norm.
- ✓ T3 specimens have a face thickness (t) of 1.2 mm and a core (c) of 6 mm, so t/c=0.20 which follow the norm.

"Also, the width should not be less than twice the total thickness, not less than three times the dimension of a core cell, nor greater than one half the span length."

- ✓ All the specimens used on these tests have 20mm of width and the maximum thickness is verified on specimens T3 with a thickness (w) of 8mm. So as l=20 and d=8, l/d= 2.5 so the length is more than twice the total thickness.

- ✓ Core cell is greater on specimen T3 with c=6 mm, so as w/c=3.33 the length of 20 mm is greater than three times the dimension of the core cell.
- ✓ The three types of specimens T1, T2 and T3 have the half of its span equals to 64, 46,5 and 80 respectively which is greater than 20 in all cases.

In order to understand easier, the geometry conditions and positioning mentioned above, figure 3.6 shows a scheme of those geometry properties.

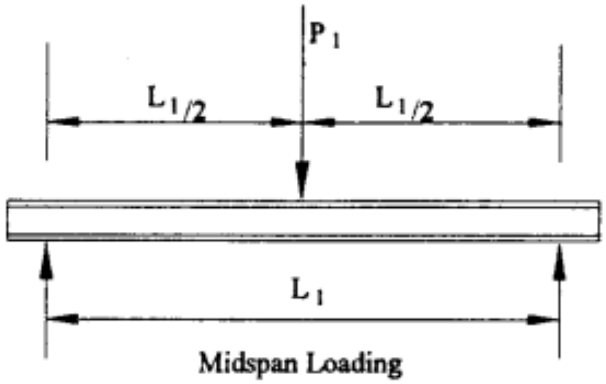

Figure 3.6- Single-point load on a three-point flexural test [32].

3.3 Experimental Tests Set-up

The equipment used to perform the tests was a universal testing machine and the software on which the testing machine was connected (figure 3.7). The testing machine was a Shimadzu AG-IS with a SPL-10kN load cell and a bench with two mounts to be used as fix points to meet the requirements of the flexural 3-point bending test.
The tests were performed using the Software *TRAPEZIUM2* Version 2.13, connected to the testing machine. To perform the three-point bending tests, a set up was required, on which the sandwich beam properties (specimens geometry) and speed test (mm/min) were inputted.

Figure 3.7 – Universal testing machine with 3 point bending test fixture mounted.

Having the Software parameters all set and ready to start, the positioning of the specimen was the next step.

First, the span length was adjusted by reducing the length between the fixed supports where the specimen will be placed using a torquing bolt and measuring the gap with the scale underneath test base, then the specimen was positioned on top of those fix points using guidance marks on the specimen to match its span length as shown on figure 3.8, making sure the full symmetry before starting the test, to verify its correct positioning. The same process was repeated for all the other types of specimens.

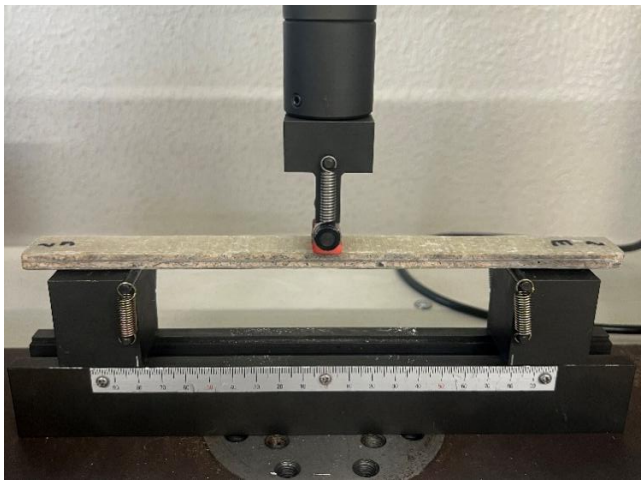

Figure 3.8- Specimen Positioning.

To avoid the crush effect (figure 3.9) made by the load cell directly on the specimen face sheet, a little piece of rubber was applied in between the loadcell touching point and the specimen face-sheet as can be seen on figure 3.8 the rubber in colour red.

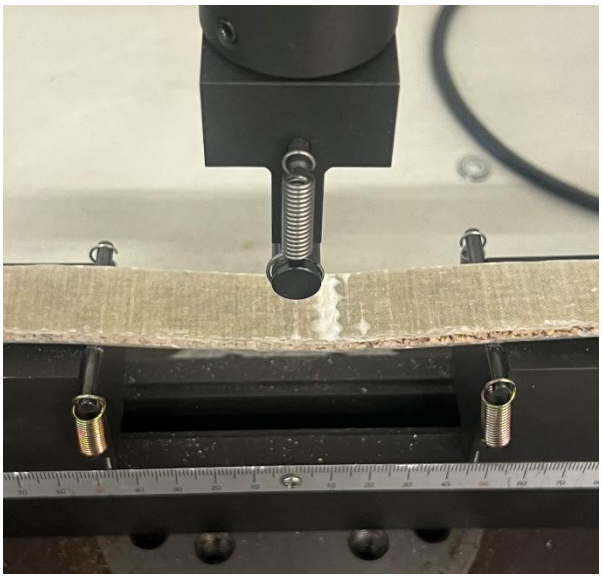

Figure 3.9 - Trial Test without protective rubber.

3.4 Experimental Results and Discussion

The results were collected by exporting each test data from the software using an excel file. The data file provided the values of Load (N) and displacement (mm) for every 0.05 seconds. The maximum load verified was experimentally obtained by observing the load at the moment immediately before it suffers the first backlash, considering this as the moment of its linear elastic regime rupture, so then the material enters a degradation phase with composite damage and cork core collapse.

In table 3.3 below, the results are presented, showing the distribution of Maximum load, time of first seen damage and test speed, for every tested specimen.

Table 3.3 - Experimental Results of Load at rupture, Time at Rupture and Speed.

Specimens	Max. Load (N)	Time at rupture (s)	Speed (mm/min)
T1 NR 3	387.87	235.15	3.25
T1 NR 4	393.57	286.6	3.25
T1 NR 5	418.85	426	2.75
T2 NR 2	360	277.7	2.5
T2 NR 3	341.90	123.9	3.75
T2 NR 4	407.25	195.05	5
T2 NR 5	375.06	183.85	3.75
T3 NR 2	573.12	242.75	3.75
T3 NR 3	542.5	197.9	4
T3 NR 4	598.75	230.8	3.75
T3 NR 5	526.06	231.6	3.75

It is also suggested by this norm that the maximum load should occur between 3 to 6 min and to do a targeting, one additional specimen was used as a trial in order to attempt to get an approximate speed to match the interval of time 3 to 6 min. The first trial test was done using an extra specimen with similar dimensions as the T2, using a load speed of 5 mm/min. The maximum load was verified 2 mins after the starting the test, which is out of the range of 3 to 6 mins. It was concluded that by reducing the load speed, the maximum force would occur later, so it was decided to start with a speed (v) of 2,5 mm/min. Several adjust on the speed were made following the behaviour of the different sets of specimens, the distribution of speed, time of test and maximum load at rupture can be seen on table 3.3 and figure 3.10 below.

It was observed that even the specimens of the same kind had a different behaviour under the same speed test, however at least one specimen of each kind had its rupture between 3 to 6 mins which was considered satisfactory to accept its experimental results.

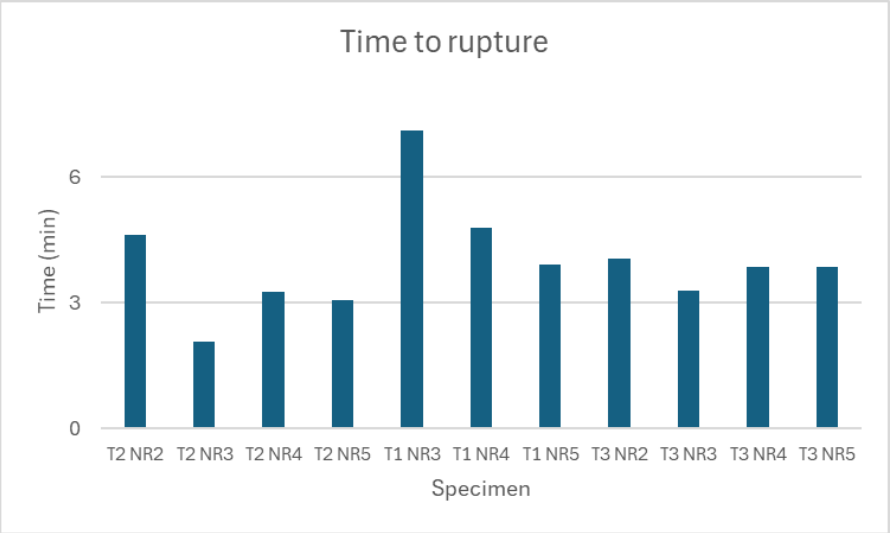

Figure 3.10 - Specimens Time to Rupture.

As observed by Bruno Soares [36] when he performed three-point bending tests on different cork cores sandwich specimens, the load-displacement curve shows an initial quasi-linear elastic regime a) macroscopic core crack appearance b); followed by a crack propagation of the specimen's extremity c).

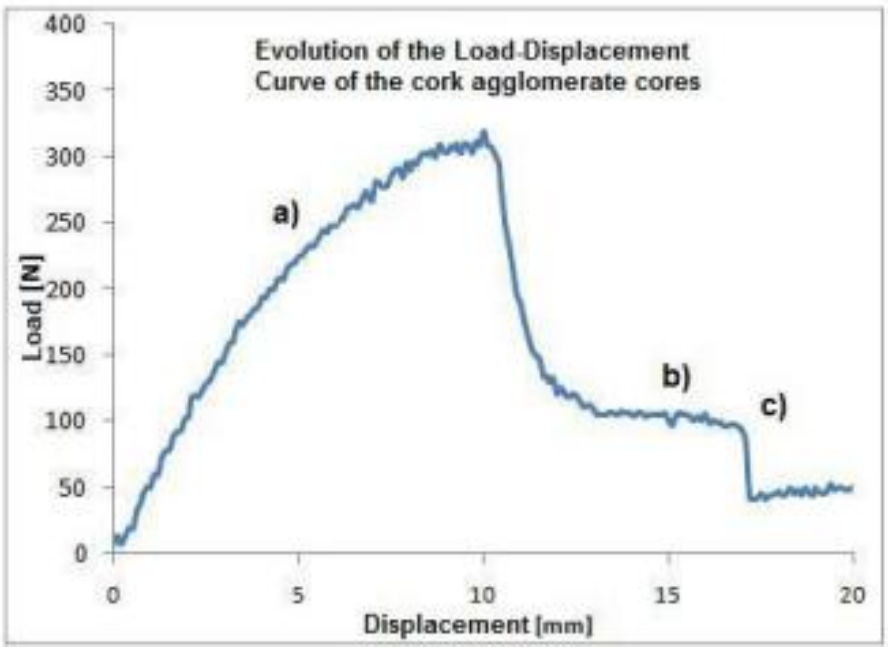

Figure 3.11 - Typical cork agglomerate Load-Displacement curve [36].

On the present study, similar curves were obtained when the experimental generated data was plotted into a load-displacement graph as shown below in figures 3.12,3.13 and 3.14:

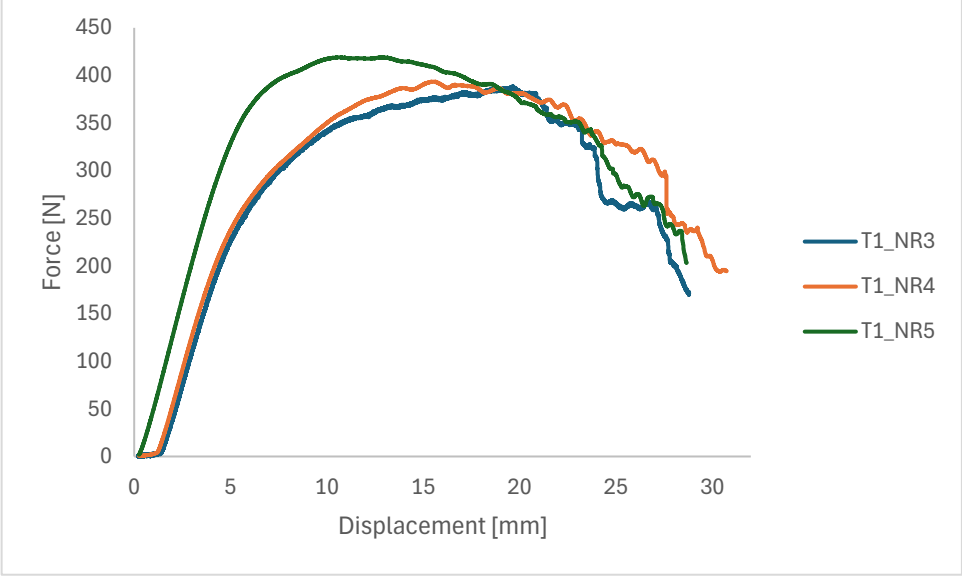

Figure 3.12 - Experimental Load-Displacement Curves for T1 Specimens.

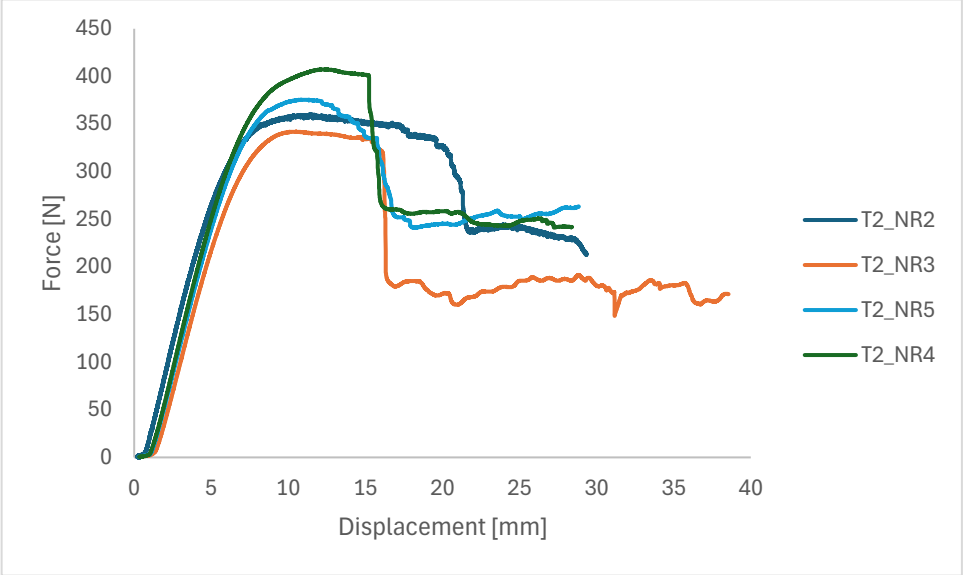

Figure 3.13 - Experimental Load-Displacement Curves for T2 Specimens.

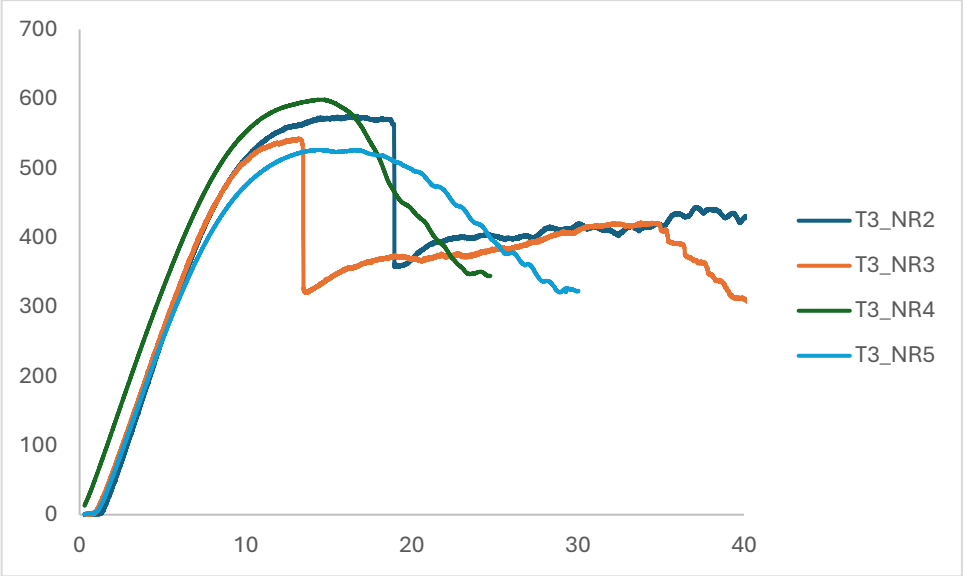

Figure 3.14 - Experimental Load-Displacement Curves for T3 Specimens.

To allow further theoretical calculations, table 3.4 below records the Maximum Load and deflection measured for each specimen test. Due to the fact that several specimens were used for preliminary test experiments and adjustments, it was not possible to have 5 specimens available for each type.

Table 3.4 - Experimental Deflection at rupture.

Specimens	Max. Load [N]	Deflection [mm]
T1 NR 3	387.87	16.84
T1 NR 4	393.31	15.41
T1 NR 5	418.85	14.42
T2 NR 2	360	11.47
T2 NR 3	341.90	10.14
T2 NR 4	407.25	12.37
T2 NR 5	375.32	10.66
T3 NR 2	574.68	16.31
T3 NR 3	542.5	13.19
T3 NR 4	598.75	14.42
T3 NR 5	525.06	14.47

3.5 Flexural Properties Calculation

ASTM C393 [35], provides equations to calculate sandwich beams flexural strength and stiffness properties. Such principles are important for better understanding the impact of the 3PB test on the sandwich beam specimens. Moreover, some of these considerations will be used to explain the obtained results.

3.5.1 Facing bending stress

Facing bending stress is the stress within the facing material of the sandwich beam, by the effect of the load applied on its surface by the 3PB test, and is calculated as follows:

$$\sigma = \frac{PmaxL}{2t(d+c)b}$$

(2.1 repeated here for convenience)

Where:

σ = facing stress (MPa)

$Pmax$ = maximum load (N)

d = sandwich thickness (mm)

c = core thickness (mm)

b = sandwich width (mm)

t = facing thickness (mm)

Using the equation (2.1), the ultimate facing bending stress was calculated for each tested specimen and such values presented on table 3.5 below:

Table 3.5 – Maximum facing bending stress.

Specimen	Ultimate Facing bending stress [MPa]
T1 NR 3	101.66
T1 NR 4	103.00
T1 NR 5	109.45
T2 NR 2	101.09
T2 NR 3	96.01
T2 NR 4	114.36
T2 NR 5	105.32
T3 NR 2	128.34
T3 NR 3	121.49
T3 NR 4	134.08
T3 NR 5	117.80

3.5.2 Sandwich beam shear rigidity

The beam shear rigidity is obtained using the core and facings dimensions and the core shear modulus. As the experimental shear stress-strain curve of the cork agglomerate used on this study was not obtained, a cork agglomerate with similar characteristics was found on the literature. Studied by Pedro Carvalho [38], the NL10 cork agglomerate shows a similar morphology compared with the cork material subject of this study, and by performing experimental shear tests in accordance with ASTM C 273 and he obtained the experimental shear modulus of 5,326 [MPa].

In this study, that value as assumed to allow the calculation of the specimens shear rigidity as given ASTM C393 [35] and presented follows:

$$U = \frac{G(d+c)^2 b}{4c} \tag{3.8}$$

Where:

U = Sandwich beam shear rigidity

G = Core shear modulus

d = sandwich thickness

c = core thickness

b = sandwich width

Using the equation (3.8), the sandwich beam shear rigidity for each tested specimen was calculation and presented on table 3.6 below:

Table 3.6 - Sandwich beam shear rigidity.

Specimen	Sandwich beam shear rigidity [N]
T1 NR 3	2299.08
T1 NR 4	2317.73
T1 NR 5	2336.47
T2 NR 2	12836.87
T2 NR 3	12836.87
T2 NR 4	12836.87
T2 NR 5	12836.87
T3 NR 2	25220.79
T3 NR 3	25220.79
T3 NR 4	25220.79
T3 NR 5	25220.79

3.5.3 Ultimate Sandwich core shear stress

The core shear stress can be calculated as given ASTM C393 [35] and presented follows:

$$\tau = \frac{Pmax}{(d + c)b} \tag{3.9}$$

Where:

τ = core shear stress

$Pmax$ = maximum load

d = sandwich thickness

c = core thickness

b = sandwich width

Using equation (3.8) the tested specimens ultimate core shear stress was calculated and presented on table 3.7 below:

Table 3.7 - Specimens core maximum shear stress.

Specimen	Ultimate Core shear stress [MPa]
T1 NR 3	2.93
T1 NR 4	2.97
T1 NR 5	3.15
T2 NR 2	1.69
T2 NR 3	1.61
T2 NR 4	1.91
T2 NR 5	1.76
T3 NR 2	2.15
T3 NR 3	2.03
T3 NR 4	2.25
T3 NR 5	1.97

3.5.4 Sandwich beam flexural Stiffness

The Flexural stiffness is given by ASTM C393 [35] and presented as follows:

$$D = \frac{E(d^3 - c^3)b}{12} \tag{3.10}$$

Where:

D = flexural stiffness

E = facing modulus

d = sandwich thickness

c = core thickness

b = sandwich width

Using the equation (3.10), the tested specimens's flexural stiffness was calculated and presented on table 3.8 below:

Table 3.8 - Specimens average flexural stiffness.

Specimen	Flexural Stiffness [N.mm2]
T1	4.06
T2	12.71
T3	24.88

3.5.5 Sandwich beam 3PB Deflection

The theoretical sandwich beam deflection under three-point bending test is given by:

$$\Delta_{3PB} = \frac{PL^3}{48D} + \frac{PL}{4U} \tag{3.11}$$

Where:

Δ_{3PB} = sandwich beam deflection

D = flexural stiffness

P = load

L = span length

Below, table 3.9 gives the theoretical calculation of the expected deflection of the sandwich beam tested and compares it with the experimental deflection obtained. It can be concluded that the experimental deflection was much higher than expected, however, the trend for both experimental and theoretical results are correlated since the highest values of deflection can be verified for T1 specimens for both theoretical and experimental and the same for T2 and T3 specimens.

Table 3.9 - Theoretical specimen deflection.

Specimen	Theoretical deflection [mm]	Experimental deflection [mm]
T1 NR 3	5.52	16.84
T1 NR 4	5.57	15.41
T1 NR 5	5.90	14.42
T2 NR 2	2.14	11.47
T2 NR 3	2.03	10.14
T2 NR 4	2.42	12.37
T2 NR 5	2.22	10.66
T3 NR 2	2.87	16.31
T3 NR 3	2.72	13.19
T3 NR 4	3.00	14.42
T3 NR 5	2.64	14.47

Considering that the formula (3.10) accounts for the maximum load when first rupture was detected and the other properties were calculated before, it can be concluded that the calculated sandwich beam stiffness calculated is higher than the real stiffness, which can be explained by the fact that the elastic modulus of the facing used was given by the manufacturer, however staking the laminates, the loads doesn't distribute perfectly so that the elastic modulus on equation (3.9) should not be exactly the same as given. However, considering the range of values obtained from both experimental and theoretical deflections that is on the same order of magnitude, those should be considered valid to get an estimation of the specimens capacities. At this point it should be considered that the deflection measured was incremented due to the fact that the cell movement was measured all the way but the rubber compression was not accounted, which resulted in a bigger measured then the real beam deflection, considering that the beam was not deflecting when the rubber was initially being compressed.

4 Numerical Analysis

This chapter aims to describe and present the numerical analysis carried out using a 2D Finite Element model using Ansys, compare it to the experimental study to discuss its similarities and discrepancies in order to present and overall analysis.

4.1 Numerical Model

A 2D FEA modelling of specimens T1, T2 and T3 was performed using ANSYS ADPL. 8-node plane solid elements (PLANE183) [37] were considered. For each specimen type, different Key points were created to mark the boundary conditions, geometry and points of interest for further mesh modelling.

Then the key points were unified by designated lines to create the material areas, on which the associated material layer was defined. To attribute different materials to the geometry to define the different layers of the specimen, a material model for each different material was created.

4.1.1 Epoxy/Fiberglass composite material properties

The epoxy/fiber glass 0º/90º reinforced laminate composite is considered an orthotropic material because there are 2 planes of symmetry at any point of the laminates. The elastic modulus of this unidirectional fiber glass/epoxy given by its manufacturer is 45 GPa [39], however as the laminates are built with 0º/90º orientation, it can be assumed as a first and quick approximation that the longitudinal modulus of the laminate 0º/90º in both longitudinal (E_x) and transversal direction (E_y) are half of its total longitudinal modulus (22.5 GPa) . Along z direction (E_z), the longitudinal modulus is equal to the matrix longitudinal modulus, which in this case it's the longitudinal modulus of the epoxy given from its manufacturer [39] (6GPa). Below table 4.1 presents the properties of the fabric used on this study.

Table 4.1 - Epoxy/Fiber-glass Laminate material properties.

Reinforced Fiber-glass material model	
E_x	22.5 [GPa]
E_y	11 [GPa]
E_z	22.5 [GPa]
v_{xy}	0.3
v_{yz}	0.09
v_{xz}	0.09
G_{xy}	6 [GPa]
G_{yz}	6 [GPa]
G_{xz}	6 [GPa]

4.1.2 Cork core material properties

The cork used as a core material on these sandwich specimens was agglomerated cork. Theoretically natural cork is considered an anisotropic material, however, the agglomerate cork can be considered as a material with the same structure in all directions, and so an isotropic material [37].

Considering that the cork elastic modulus was not given by the manufacturer and the tensile tests were not performed on this study, the elastic modulus of a similar cork agglomerate considering its grain sizing and cork grade was obtained by Paulo Carvalho [38] an assumed for calculation purposes on this study.

With this assumption the material model for cork. was created given the following properties:

Table 4.2 - Cork core material properties [38].

Cork Material Model	
E_x	16 [MPa]
v_{xy}	0.01

Besides the material definition, the material areas were also defined with the objective to set meshing boundaries. as different meshing settings were applied pending on the specimen's zone. For example, the area that was expected to deflect more was set with a more refined mesh and the same logic was considered for the highest load propagation zones. Below it can be observed as an example the T1 specimen with a more refined mesh around the point on which the force is applied marked with the red arrow and the

point of highest deflection around the axis origin (showing z axis facing the screen as this is a 2D model).

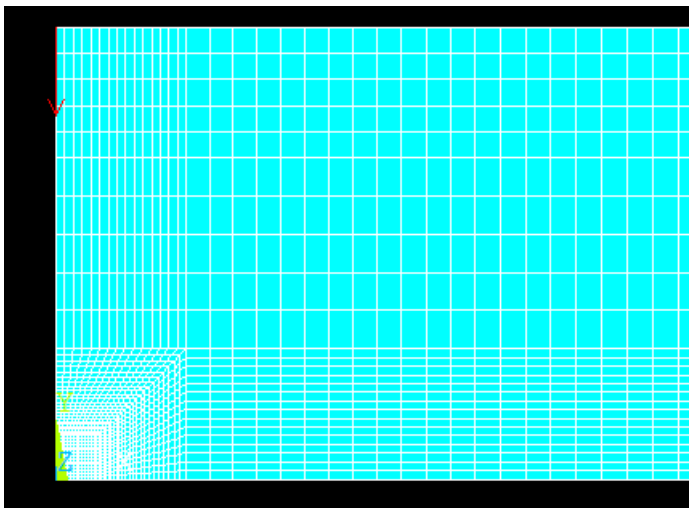

Figure 4.1 - T1 Specimen Meshing setting.

The boundary conditions were set to simulate the three-point bending test in accordance with the body diagram below presented by figure 4.2, on which the load (Fmax) was the maximum load that each specimen experienced before plastic rupture. The point of contact with the mount is in this case at L/2 instead of L due to the reason that software is considering half of the specimen using its symmetry, so the L dimension was then divided in half and same logic was considered for Fmax, so that Fmax was divided by two.

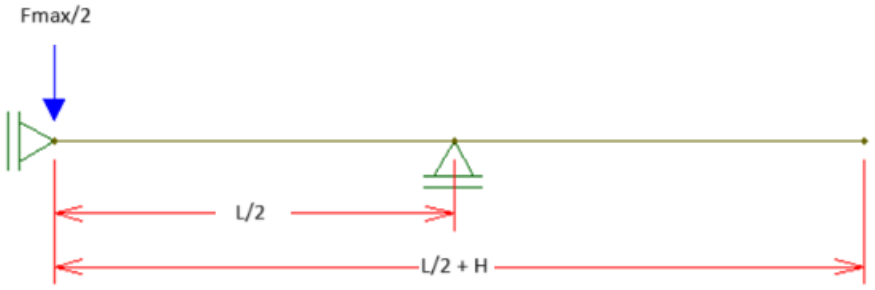

Figure 4.2 - Three-point bending numerical test body diagram.

The Ansys software screenshots below, shown that the boundary conditions and meshing were well implemented and in accordance with the FEM. It can be seen that the geometry is describing a curve mostly between the point of Load application and the fixed support at L/2. This shows the similarity between the experimental flexural behaviour and the numerical flexural analyses.

4.1 Numerical Results

As mentioned, the numerical study was performed on based on the FEM model which can only consider the linear elastic regime of the flexural tests. Hence, the numerical analyses were performed considering the linear elastic regime only, using the maximum loads obtained experimentally for that regime. Table 4.3 below, presented the yield loads obtained experimentally and considered for the numerical analysis.

Table 4.3 - Linear elastic regime maximum loads.

Specimen	Applied FEM Load [N]
T1 NR 3	260
T1 NR 4	262
T1 NR 5	340
T2 NR 2	313
T2 NR 3	299
T2 NR 4	358
T2 NR 5	331
T3 NR 2	438
T3 NR 3	434
T3 NR 4	505
T3 NR 5	404

Using the FEM loads as per table 4.3, the simulations were finally performed for each specimen type model. Those simulations are shown below (figure 4.3, figure 4.4 and figure 4.5) on which a similar deflection geometry and flexural behaviour when compared to the experimental tests can be observed.

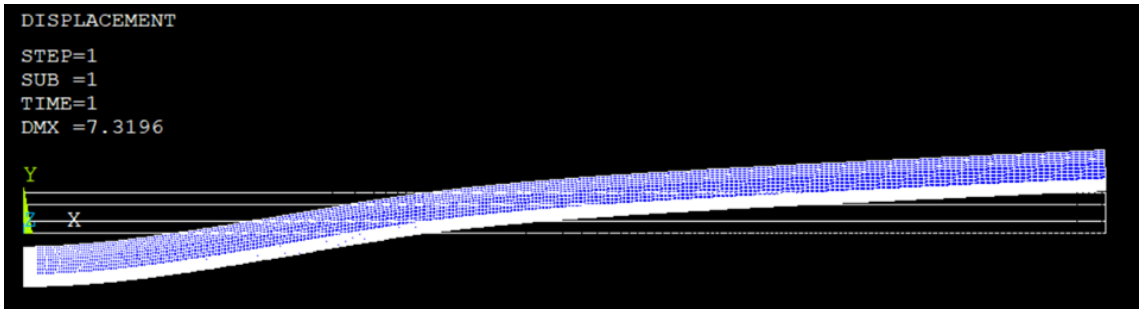

Figure 4.3 - Three-point bending numerical result of Specimen T1.

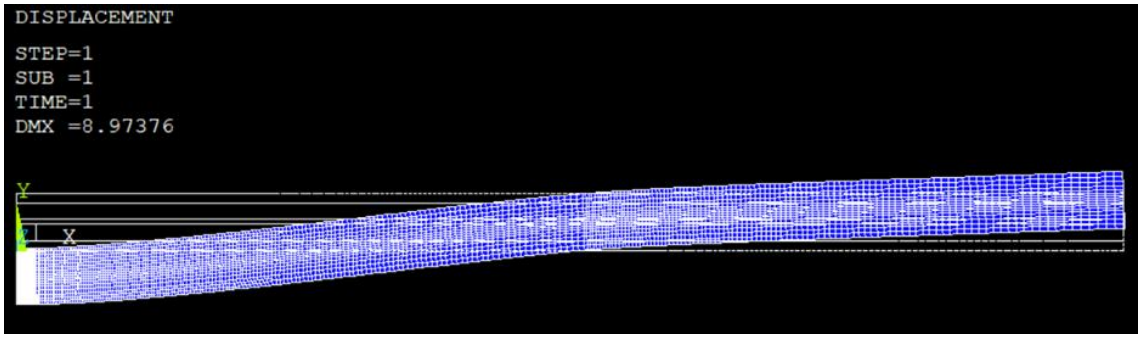

Figure 4.4 - Three-point bending numerical result of Specimen T2.

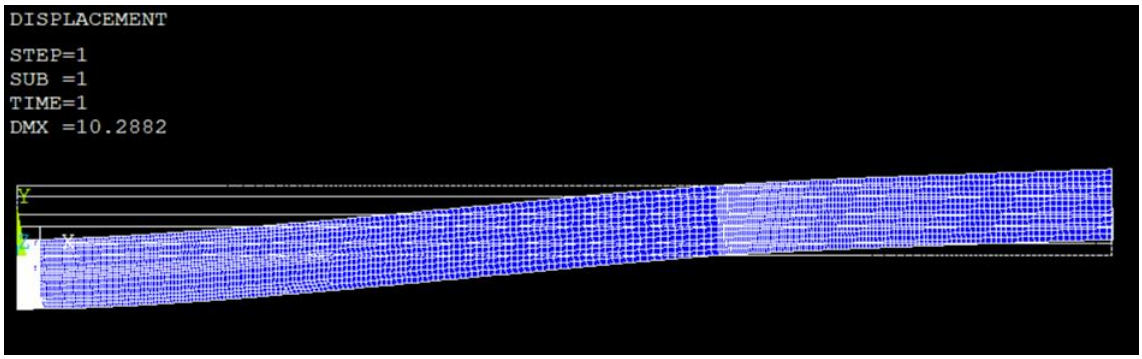

Figure 4.5 - Three-point bending numerical result of Specimen T3.

For comparison with the experimental results, the Force-Displacement Curves obtained from experimental results, and the FEM solution obtained from the numerical calculation, were plotted and presented by figure 4.6, figure 4.7 and figure 4.8 below:

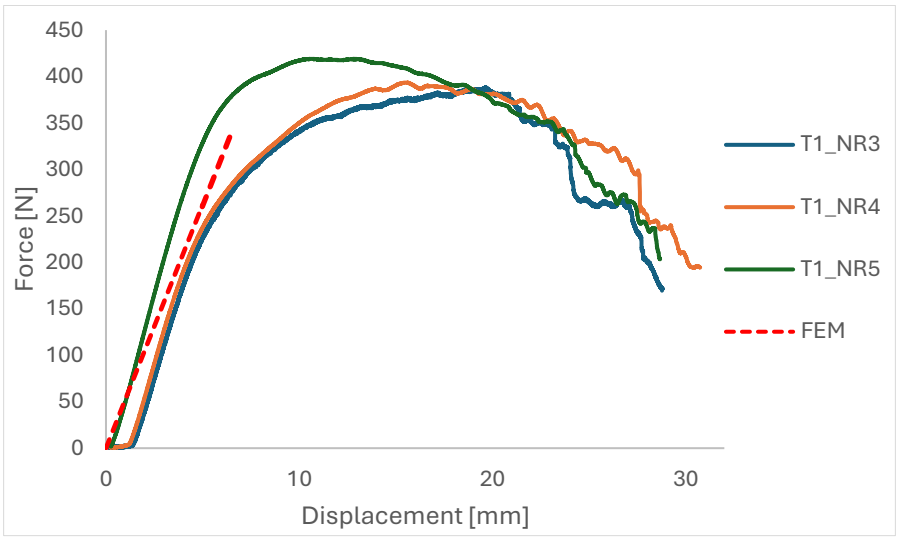

Figure 4.6 - T1 Experimental and Numerical Results.

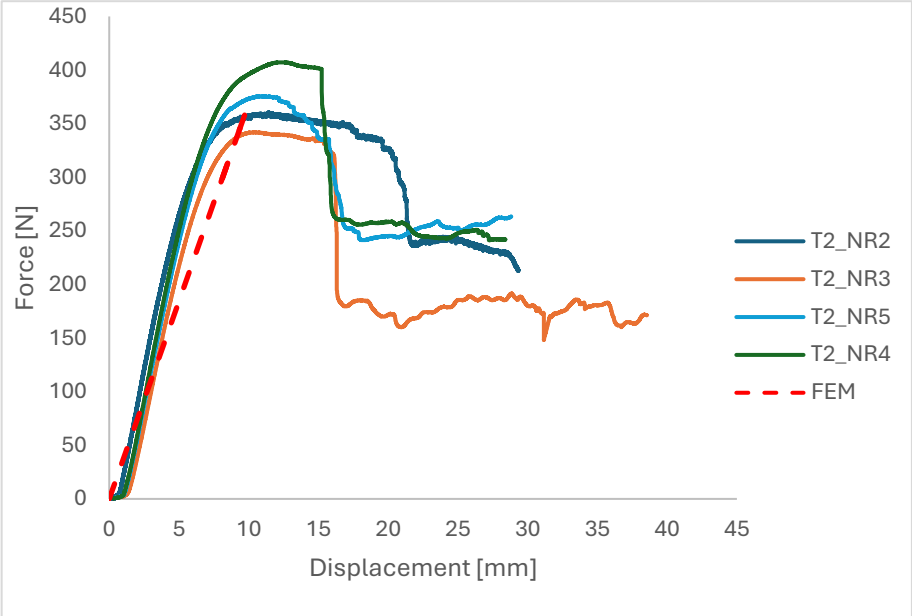

Figure 4.7 - T2 Experimental and Numerical Results.

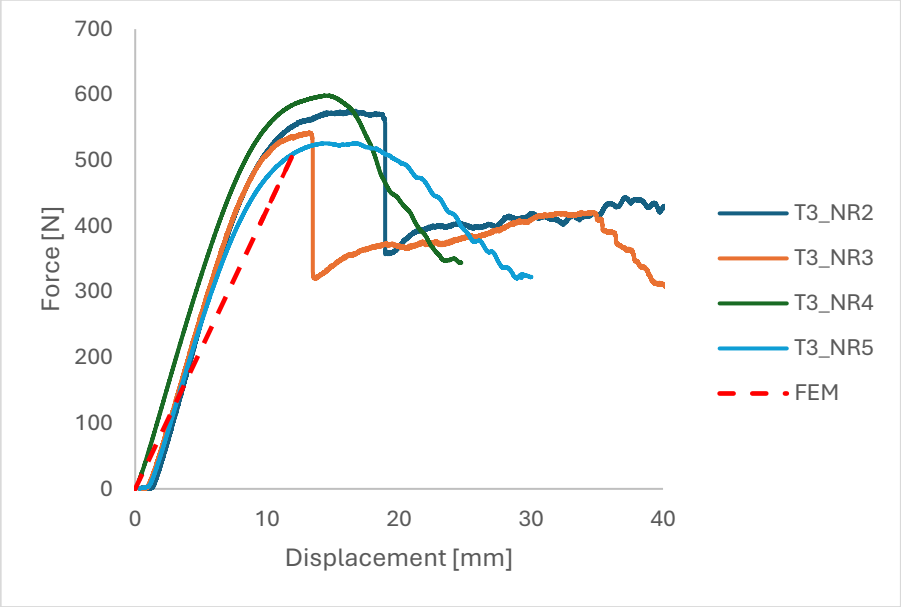

Figure 4.8 - T3 Experimental and Numerical Results.

The FEM solution on all graphs, shows that the numerical calculation is trending the experimental data so that it can be considered that the numerical modelling is valid, however, there are a visible discrepancy between FEM and experimental results, which can be explained by the assumptions there were done for material properties such as reinforced cork agglomerate and reinforced epoxy/fiberglass materials elastic modulus.

5 Failure Modes Analysis

On this chapter, the results obtained and the failure modes of the specimens tested are presented and discussed. Pictures of the specimens upon the 3PB tests were shown and referred to the graphs obtained on chapter 4, global considerations and conclusions are made.

5.1 T1 Specimens analysis

On T1 specimens, it was observed a core failure and similar behaviour and results on all of the set. The failure mode shown a smooth and slow crack initiation and progression from the load point to the extremity of the specimen, allowing the load to maintain high for a long time, without significant drops on the initial phase of the plastic regime, which is represented by a smooth curve observed on figure 4.6 and also from the photo on figure 5.1 below.

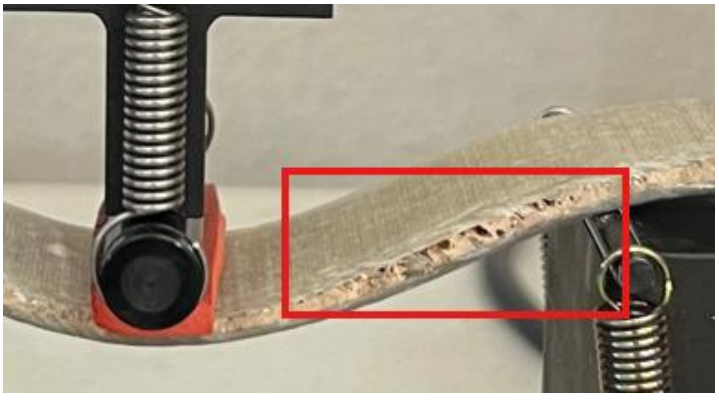

Figure 5.1 - T1 specimen core crack.

The T1 Nr2 and Nr3 specimens presented almost the same maximum load of 260 and 262 N respectively, however the Nr.5 presented a discrepancy on the load registered. There are many reasons that could affect the discrepancy on the maximum load registered for this specimen, such as material manufacturing issues like the presence of

spots of resin spots in the middle of the cork agglomerate technical aspects during the 3PB test execution, in this case the reduced speed test used of the 2.75mm/min instead of 3.25mm/min used on the other T1 specimens.

5.2 T2 Specimens analysis

With regards to the load-displacement curve, a slight difference was observed on T2 specimens, on which it can be seen for all specimens curves presented on figure 5.2 that was a significant load decrease at the moment of its rupture. This can be explained by the fracture of the interlayer of reinforced epoxy/fiberglass. Theoretically, T2 specimens experienced a lower shear stress when compared with T1 specimens, this can be assumed as the reason why the cracks opened on its core at rupture and much smaller and contained then on T1 specimens as can be seen of figure 5.1. This can be explained by the presence of the interlayer of reinforced fiberglass, impending the deformation tensions through the thickness reducing the core shear stress as can be confirmed by the calculation and results from chapter 3.5

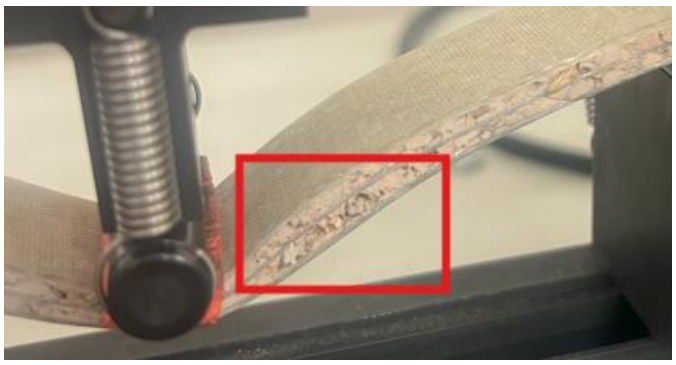

Figure 5.2 - T2 Specimen core failure.

Even though that the three specimens of T2 set, Nr 2 Nr3 and Nr4 presented distant load values between each other of 360, 341 and 407 N respectively, as per figure 4.7 it can be observed that the behaviour of its curves was similar and within an acceptable trend.

5.3 T3 Specimens analysis

For T3 specimens, it was observed that the upper facing of the specimen crushed before the core failure as per figure 5.3, which means that the compressive stress on the sandwich beam on its compression facing was the failure mode of this specimen, contrary to the failure modes on specimens T1 and T2, in this case the core shear stress was not enough to fracture the core. This can be explained by the difficulty of bending

the specimen due to its higher thickness, increasing the tensile stress on specimen's facing.

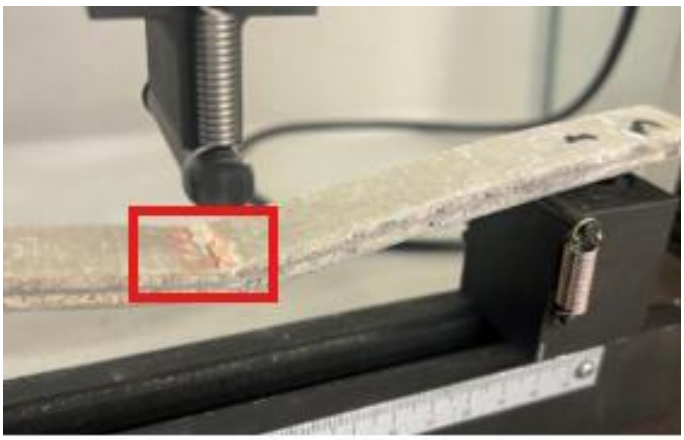

Figure 5.3 -T3 specimen crushed facing.

It can be seen that on figure 4.8 that the load-displacement curves for the T3 set of specimens are similar and almost identical on the linear elastic regime, there was also variation of the maximum load and displacement recorded, which as mentioned already for other specimen types, has to do with material/manufacturing process issues and also the test speed difference. Considering the calculations on chapter 3, it was expected to obtain a higher sandwich flexural stiffness and higher ultimate stresses at the time of rupture due to its higher thickness when compared with the other two sets of specimens T1 and T2, which was verified on the experimental test.

6 Comparison with other materials

To do an evaluation of the sandwich beam types subject of this study, it is relevant to compare the results obtained with other sandwich beams made of different materials, tested with a 3PB in accordance with ASTM C393, same as performed on this study. the table 6.1 below shows the general experimental results and calculations obtained on previous chapters.

Table 6.1 – Flexural Tests Global Results.

Specimen	Maximum Facing bending stress, σ [MPa]	Maximum Core shear stress, τ [MPa]	Sandwich bending stiffness, D [N.mm^2]	Maximum Load, L [N]	Displacement, Δ [mm]
T1 NR 3	101.66	2.93	4.06	387.87	16.84
T1 NR 4	103.00	2.97	4.06	393.31	15.41
T1 NR 5	109.45	3.15	4.06	418.85	14.42
T2 NR 2	101.09	1.69	12.71	360	11.47
T2 NR 3	96.01	1.61	12.71	341.90	10.14
T2 NR 4	114.36	1.91	12.71	407.25	12.37
T2 NR 5	105.32	1.76	12.71	375.32	10.66
T3 NR 2	128.34	2.15	24.88	574.68	16.31
T3 NR 3	121.49	2.03	24.88	542.5	13.19
T3 NR 4	134.08	2.25	24.88	598.75	14.42
T3 NR 5	117.80	1.97	24.88	525.06	14.47

It is important to clarify that the values of deflection shown below are the experimental values and all the calculations were done using the maximum load measured for each specimen under 3PB test when the failure occurred.

Pedro Carvalho [38] performed a 3PB test as per ASTM C393, on different sets of specimens using different cork agglomerates (NL10, NL30) and facings of fiberglass. Below is presented the distribution of his tested specimens configuration.

Bruno Soares [36] also performed the same test methodology on different sets of sandwich beams made of different cork agglomerates (CAI-8810, CAI-8123, CAI-8303), Honeycomb and Rohacell 51 cores with facings of carbon fiber.

Both authors presented the average results obtained per set of specimens, therefore, the average results of this study were also calculated and presented on table 6.2 below.

Table 6.2 - Comparison between T1, T2 and T3 results with different sandwich beam results from other studies.

Sandwich beam	**Maximum Facing bending stress, σ [MPa]**	**Maximum Core shear stress, τ [MPa]**	**Sandwich bending stiffness, D [KN.mm^2]**
NL10 [36]	17,613	0.203	4.853
NL30 [36]	14.024	0.16	7.141
CAI-8810 [36]	18.592	0.173	14.815
CAI-8123 [36]	23.534	0.311	45.906
CAI-8303 [36]	12.316	0.201	60.265
Rohacell 51 [38]	72.230	0.945	84.397
Honeycomb [38]	76.782	1.2	172.076
T1	104.7	3.01	4.06
T2	104.2	1.74	12.71
T3	125.42	2.1	24.88

Analysing the table 6.2 above, it can be concluded that sandwich beams subject of this study T1, T2 and T3 presented acceptable results when compared to the other sandwich materials, more precisely compared with the other sandwich specimens with cork agglomerate cores. Rohacell 51 and Honeycomb are still the best solution when it comes to bending stiffness as expected. However, all these results are directly related with the configuration of each specimen, as presented on chapter 3, the core and facing thickness had a direct relation with shear and facing stress respectively. However, as stated by Pedro Carvalho [38], the results should not be assessed independently but as a result of the sandwich beam material interaction, so a straight comparison between two different sandwich materials from different specimens is risky but provides evidence of quality standards matching the range of values obtained which was verified.

7 Conclusions and Future works

7.1 Conclusions

In an overall analysis of this study, it was concluded the following relevant points that should be highlighted:

Considering that globally except for T3 specimens, core failure was the most observed failure mode, and all of the specimens presented different crack propagation length and size, it can be pointed out that the agglomerated cork material should be more refined with smaller grain sizing, reducing the empty spots or excess spots of resin thought its thickness and length.

Among the three types of specimens tested, it can be concluded that in shear, T3 performed much better than the others considering it sustained the integrity of its core as mentioned. T1 presented the lowest shear strength and the lowest stiffness, however its yield stress was not radically different from the other two types. T2 specimens shown that its flexural strength and stiffness were not much better then T1, which due to its more complex manufacturing process requiring the use of a fabric interlayer and the extra material spent for that purpose would not be selected in lieu of T1 sandwich beam, Considering that T1 is a cheapest solution due to much easier manufacturing process and less material utilization, it can be considered as the more suitable solution for the majority of the applications.

The manual manufacturing process, by being performed on different days on a open atmosphere allowing the influence of temperature variations, had a visible impact on the cure quality specially on the reinforced fiber glass facings by the appearance of color tons on its surface.

The experimental 3PB tests, were performed using a rubber between the load cell contact point and the specimen which had a compressing effect that was not assessed and accounted on the load-displacement results. When the load cell establishes contact with the rubber, it started to compress and immediately the software starts counting the load cell movement, measuring the displacement, however the specimen is doesn't start to bend immediately. In this case, the use of an extensometer positioned below the specimen would be the best way to measure the real displacement of the experimental 3PB test instead of the load cell movement measurement which inducts considerable error on the displacement measurement.

Cork agglomerate core with reinforced fiberglass facings, proved to perform with similarity and better and some cases when compared with other material more commonly used nowadays on engineering applications, however as discussed, morphologic wise, cork as a cellular material with randomly distribution of its cell it is still a hard material to be standardized and dimensioned for engineering purposes, this explains the fact that it is still not widely compared with other materials despite its outstanding advantages.

7.2 Future Works

It was pointed out that some improvements such as proper material construction using advanced tools and a proper vacuum machine instead of weight blocks and open atmosphere would provide a more reliable and uniform specimens.

As well for the experimental procedure, the displacement measurement that should be done using an extensometer, the utilization of a rubber between the load cell and the specimen without load absorption calculation and speed test uniformization for all tests could be made on the experimental procedure and manufacturing process, which should be implemented on future works in order to obtain more accurate and reliable results.

In addition, in order to have a proper overall data and analysis, the sandwich specimens should be subject to tensile, compressive and shear tests in accordance with ASTM C 297, ASTM C 364 and ASTM C 273 respectively.

Specially cork agglomerate core should be subject to shear test in order to obtain its stress-strain curves and calculate the core shear modulus which in this study was assumed per similar studies in the literature.

The design criteria for tensile and compressive strength should be of using the reverse considerations given in ASTM C363, targeting a specify range of results in advance.

Using sets of different cork agglomerate cores on the experimental tests is also a relevant criteria, which in this case was considered to be a miss criteria as there was no other cork agglomerate type to compare the specimens with.

To address the fiber-matrix relation in terms of volume in relation to its strength, different sets of specimens with various fiber-matrix volumes can be manufactured in order to test and obtain the best solution for sandwich beam performance.

A 3D FEM numerical analysis would provide a better visibility and relevant information regarding the tensile and shear stress localization, its propagation and crack growth.

Summarizing, all the improvements above should be done on future studies. Moreover, ideally, a small scaled engineering application such as aircraft wing-to-body fairy composite panel, should be tested along the proposed sandwich cork solution and compared its performance, a supply-chain and manufacturing costs and viability study should be included in order to outcome with a realistic industrial applicability conclusion.

References

[1] R. M. Jones (1999). CRC Press. Mechanics Of Composite Materials (2nd ed.).httpsdoi.org10.12019781498711067

[2] Egbo, Munonyedi. (2020). Journal of King Saud University - Engineering Sciences. A fundamental review on composite materials and some of their applications in biomedical engineering

[3] Ngo, TriDung (T.-D.). (2020*). Introduction to Composite Materials*. 10.5772intechopen.91285

[4] M.K.S.Sai. (2016). International Journal of Latest Trends in Engineering and Technology (IJLTET). *Review on composite classification. manufacturing. and applications*. http://www.ijltet.orgjournal1

[5] Alemour, Belal & Badran, Omar & Hassan, Mohd. (2019). Journal of Aerospace Technology and Management. *A Review of Using Conductive Composite Materials in Solving Lightening Strike and Ice Accumulation Problems in Aviation*. 11. 10. 5028jatm.v11.1022.

[6] Gay D, Suong V, Hoa. Stephen, W. Tsai. (2002). CRC Press. *Composite Materials: Design and Applications*

[7] Stephen W, Tsai. (1996). Technical Report AFML-TR-66-149 PART1.*Mechanics of Composite Materials*

[8] S. Rana, F. Raul. (2016). Woodhead publishing Series in Composites Science and Engineering Number 70. *Advanced Composite Materials for Aerospace Engineering*

[9] Diab (2018). *Guideline to core and Sandwich*. http://www.diabgroup.com

[10] H. Altenabach, J. Altenbach, W. Kissing. (2004) Springer-Verlag Berlin Heidelberg GmbH *Mechanics of Composite Materials*.10.1007/978-3-662-08589-9

[11] A. Brent Strong. (2008). Fundamentals of Composite Manufacturing – Materials, Methods and Applications, Second Edition

[12] Silva, Susana & Sabino, Marcos & Fernandes, Emanuel & Correlo, Vitor & Boesel, Luciano & Reis, Rui L. (2005). International Materials Reviews. *Cork Properties. capabilities and applications*. 50. 345-365.

[13] L. Gil. (2009). Apcor - Associação Portuguesa de Cortiça. *A cortiça como material de construção – Manual Técnico*

[14] Sen. Ali & Quilhó, Teresa & Pereira, Helena, (2011). Industrial Crops and Products - IND CROPS PRODUCTS. *The cellular structure of cork from Quercus cerris var. cerris bark in a materials' perspective*. 34. 929-936. 10.1016/j.indcrop.2011.02.015

[15] Apcor.com (2023). O Setor da cortiça. Caracterização diagnóstico tecnológico estratégia Available: www.apcor.com

[16] Apcor.com (2015). *Manual técnico de Rolhas*. Available: www.apcor.com

[17] Pereira, Helena, M. Emília Rosa, M.A. Fortes. (1987). IAWA Journal 8. 3. 213-218. *The Cellular Structure of Cork from Quercus Suber L*. httpsdoi.org10.116322941932-90001048

[18] Veras M. (2013) Instituto Superior de Engenharia de Lisboa, Master Thesis - *Estudo. Fabrico e Caracterização de Painéis Sanduíche com Núcleos em Materiais Compósitos de Cortiça*

[19] Parralejo, A. D. Guiberteau, F.. Fortes, M. A.. & Rosa, M. E. (2001). Revista De Metalurgia. 37(2*)* 330–335*. Mechanical properties of cork under contact stresses*

[20] P. Fernández, Boher, P Soler. M. et al. (2021). Sci Rep 11. 12053. Transcriptomic analysis of cork during seasonal growth highlights regulatory and developmental processes from phellogen to phellem formation. https://doi.org/10.1038/s41598-021-90938-5

[21] Gibson L, J. Easterling, K. E. and Ashby M. (1981). Proc. R. Soc. Lond. A37799–1171. *The structure and mechanics of cork*

[22] Moreira, R.A.S. & Melo, Francisco & Rodrigues. J. (2010). Journal of Materials Science. 45. 3350-3366. *Static and dynamic characterization of composition cork for sandwich beam cores*

[23] Gerometta, Massimiliano & Gabrion, Xavier & Lagorce-Tachon, Aurélie & Thibaud, Sébastien & Karbowiak, Thomas. (2023). *Towards better understanding of the strain–stress curve of cork: A structure–mechanical properties approach.* Materials & Design. 235. 112376. 10.1016/j.matdes.2023.112376

[24] Lopes, João & Silva, Arlindo & Reis, Luis. (2007). Bending Tests of sandwich specimens containing cork agglomerates – comparison with other materials. Conference: Materiais 2007, Porto, Portugal

[25] Silva, José & Devezas, Tessaleno & Silva, Arlindo & Gil, Luis & Nunes, C. & Franco. N. (2010). Materials Science Forum - MATER SCI FORUM. *Exploring the Use of Cork Based Composites for Aerospace Applications.* 636-637. 260-265. 10.4028/www.scientific.net/MSF.636-637.260

[26] Daniel, Isaac & Gdoutos, E. (2010). *Failure Modes of Composite Sandwich Beams.* 10.1007_978-90-481-3141-9_9

[27] Rosário I. (2019). Instituto Superior Técnico. Master Thesis - *Viability Study for a Carbon-Cork Sandwich Composite*

[28] Selvarayan, Sathis & Milwich, Markus & Deopura, Bl & Planck, Heinrich. (2011). Procedia Engineering. *Finite element analysis of Carbon composite sandwich material with agglomerated Cork core*

[29] Peixoto D. (2017) Universidade da Beira Interior. Master Thesis - Sandwich *Cork Agglomerate Cores for Thermal Insulation Purposes in Aircraft*

[30] Muralidharan, B & Subbu, S & K Ajikumar, Arjun & Koonapalli, Thejesshanand & Sasidharan, S. (2025). Engineering Research Express. *Experimental and numerical study of three-point bending test in five different FDM 3D printed PLA core with carbon fiber sandwich structures.* 7. 10.1088/2631-8695/adc0e5

[31] Thomsen, O.T. (1991). Special Report No. 7, Institute of Mechanical Engineering, Aalborg University, Denmark. *Flexural Response of Sandwich Panels Subjected to Concentrated Loads*

[32] Zenkert D. (1997) - *The Handbook of Sandwich Construction*

[33] W.G. Heath (1960). Aircraft Eng. Sandwich construction, Part 2: *The optimum design of flat sandwich panels.* 32, 230-235

[34] N. J. Hoff, and S.E. Mautner. (1945). J. Aero. Sci., 12. *The buckling of sandwich-type problems,* 285-297

[35] ASTM (20209. ASTM C393*. Standard Method for Core Shear Properties of Sandwich Constructions by Beam Flexure*

[36] Soares B. (2007). Instituto Superior Técnico, Master Thesis- *Estruturas Sandwich com Utilização de Núcleos de Cortiça*

[37] Thirumump *et al*. (2015). Journal of Engineering and Applied Sciences. *A numerical study of SCF convergence using ansys*

[38] Carvalho P. (2008). Instituto Superior Técnico, Master Thesis - *Análise do Comportamento e Identificação do tipo de falha em estruturas sandwich com núcleos de cortiça*

[39] Leite A. (2008). Instituto Superior Técnico, Master Thesis – *Flexão de Elementos Curvos em Materiais Compósitos*

Appendix 1 - Ansys Numerical FEM Model 2D – T1 Specimen's

```
/CLEAR,START
/PREP7
!T1 SPECIMEN

! VARIAVEIS


LT = 250              !total length span
L = 93                    !length between the supports


! 5F/1C/5F TOTAL THICKNESS=4.65

H1 = 1.34                        ! 5F - Fibra Vidro  (5 camadas de 0.2675mm)

H2 = 1.97                       ! 1C - Cork Core Thickness

H3 = 1.34                        ! 5F - Fibra Vidro  (5 camadas de 0.2675mm)

SIZE_SQ = H3/3  ! ESP DE H3 / 3


! EL TYPE - 8 NOS
ET,1,PLANE183
!*
```

```
KEYOPT,1,3,3                    ! 0, TP, 2 - DP, 3 - PL STRESS W THICKNESS
R,1,20

!#####################################################################
#################

! MATERIAIS



MPTEMP,,,,,,,,
MPTEMP,1,0
MPDATA,EX,1,,22.5E3          ! MPa 1 - Resina/Fibra de Vidro
MPDATA,EY,1,,11E3
MPDATA,EZ,1,,22.5E3
MPDATA,PRXY,1,,0.3
MPDATA,PRYZ,1,,
MPDATA,PRXZ,1,,
MPDATA,GXY,1,,6E3
MPDATA,GYZ,1,,6E3
MPDATA,GXZ,1,,6E3


MPTEMP,,,,,,,,
MPTEMP,1,0
MPDATA,EX,2,,16              ! MPa  2 - Cortiça
MPDATA,PRXY,2,,0.01


MPTEMP,,,,,,,,
MPTEMP,1,0
MPDATA,EX,3,,22.5E3          ! MPa 3 - Resina/Fibra de Vidro
MPDATA,EY,3,,11E3
MPDATA,EZ,3,,22.5E3
MPDATA,PRXY,3,,0.3
MPDATA,PRYZ,3,,
MPDATA,PRXZ,3,,
```

```
MPDATA,GXY,3,,6E3
MPDATA,GYZ,3,,6E3
MPDATA,GXZ,3,,6E3


!#########################################################################
################

!PONTOS


K,1,
K,2,SIZE_SQ ,
K,3,H3,

K,4,L/2,

K,5,LT/2,
K,6,LT/2,H3,

K,7,L/2,H3,

K,8,H3,H3,
K,9,0,H3,
K,10,0,SIZE_SQ ,
K,11,SIZE_SQ ,SIZE_SQ ,

K,12,LT/2,H3+H2,

K,13,L/2,H3+H2,
K,14,H3,H3+H2,

K,15,0,H3+H2,

K,16,LT/2,H3+H2+H1,

K,17,L/2,H3+H2+H1,
K,18,H3,H3+H2+H1,
```

K,19,0,H3+H2+H1,

!###
#########

!LINES

L,1,2
L,2,3
L,3,4
L,4,5
L,5,6
L,7,6
L,8,7
L,9,8
L,10,9
L,1,10
L,10,11
L,11,8
L,2,11
L,3,8
L,4,7

L,6,12
L,7,13
L,8,14
L,9,15

L,13,12
L,14,13
L,15,14

L,12,16
L,13,17
L,14,18
L,15,19

```
L,17,16
L,18,17
L,19,18

!#########################################################################
###

!AREAS

AL,1,13,11,10   ! SIZE_SQ
AL,2,14,12,13   ! TRAPEZIO DTO
AL,11,12,8,9   ! TRAPEZIO ESQ
AL,8,18,22,19 ! 1ª ESP DA EPOXI
AL,22,25,29,26  ! 1ª H1
AL,3,15,7,14    ! 2ª H2
AL,7,17,21,18   ! 2ª ESP DA EPOXI
AL,21,24,28,25  ! 2ª H1
AL,4,5,6,15     ! 3ª H2
AL,6,16,20,17 ! 3ª ESP DA EPOXI
AL,20,23,27,24          ! 3ª H1

/PNUM,KP,1
/PNUM,LINE,1
/PNUM,AREA,1

!#########################################################################
#################

!MALHAS



!MALHA
NDIV = 15
ESP = H3/NDIV  ! H3 É A ESPESSURA DO MAT 2 DE BAIXO

! MALHA A1 SQUARE
```

```
KESIZE,1,SIZE_SQ/NDIV     ! SIZE_SQ É H3/3
KESIZE,2,SIZE_SQ/NDIV
KESIZE,11,SIZE_SQ/NDIV
KESIZE,10,SIZE_SQ/NDIV


!A2 E A3 AREAS TRAPEZOIDES

KESIZE,3,ESP ! OU SEJA ELEMT 3X MAIORES DO QUE SIZE_SQ. ESP = H3/NDIV.
SIZE_SQ/NDIV = H3/3NDIV
KESIZE,8,ESP
KESIZE,9,ESP

KESIZE,14,ESP
KESIZE,15,ESP

! 0 - FREE MESHING; 1 - USE MAPPED MESHING

MSHAPE,0              ! 0 - USE QUADRILATERALS,  1 - USE TRIAGLES
MSHKEY,1              ! MAPPED

!MALHA A2 E A3

AATT, 3
AMESH,1
AMESH,2,3,1


! MALHAR A4

LESIZE,8,ESP
LESIZE,18,H2/5
LESIZE,19,H2/5
LESIZE,22,1*ESP

AATT, 2
AMESH,4
```

```
!MALHAR A5

LESIZE,26,H1/5
LESIZE,25,H1/5
LESIZE,29,1*ESP

AATT, 1
AMESH,5

!MSHAPE,0

!MALHAR A6 E A7 E A8

LESIZE,3,,,130,2
LESIZE,7,,,130,2
LESIZE,21,,,130,2
LESIZE,28,,,130,2


LESIZE,17,H2/5

LESIZE,24,H1/5

LESIZE,23,,,4,1


AATT, 3
AMESH,6

AATT, 2
AMESH,7

AATT, 1
AMESH,8


!MALHAR A9, A10 E A11
```

```
LESIZE,23,H1/5
LESIZE,16,H2/5
LESIZE,4,,,150,2
LESIZE,6,,,150,2
LESIZE,20,,,150,2
LESIZE,27,,,150,2


AATT, 1
AMESH,11

AATT, 2
AMESH,10

AATT, 3
AMESH,9

!CONSTRAGIMENTOS


DL,10, ,SYMM
DL,9, ,SYMM
DL,19, ,SYMM
DL,26, ,SYMM
DK,4,UY,0

!#########################################################

!FORÇAS


FK,19,FY,MAXLOAD/2     ! Força máxima observada no ensaio


FINISH
/solu
!ANTYPE,0
!NLGEOM,1
```

```
SOLVE

FINISH
/POST1

PLDISP,2
```

Appendix 2 - Ansys Numerical FEM Model 2D – T2 Specimen's

```
/CLEAR,START
/PREP7
!T2 SPECIMEN

! VARIAVEIS

LT = 250                    !total length span
L = 128                     !length between the supports

MAXLOAD = -360 ! MAX LOAD SPECIMEN T2_NR2

! A - E

! 4F/1C/2F/1C/4F  TOTAL THICKNESS=6.4

H1 = 1.07                   !4F  - Fibra Vidro (4 Camadas de 0.2675)

H2 = 1.863                      !1C  - Cork Core

H3 = 0.535                  !2F  - Fibra Vidro (2 camadas de 0.2675)

H4 = 1.863                      !1C  - Cork Core

H5 = 1.07                   !4F  - Fibra Vidro (4 Camadas de 0.2675)


SIZE_SQ = H5/3  ! ESPESSURA DO MAT DE BAIXO / 3
SIZE_SQ1 = 2*H5 ! DOBRO DA ESPESSURA DO MAT DE BAIXO


! EL TYPE - 8 NOS
ET,1,PLANE183
!*
```

```
KEYOPT,1,3,3                    ! 0, TP, 2 - DP, 3 - PL STRESS W THICKNESS
R,1,20

!#########################################################################
#########

! MATERIAIS:


MPTEMP,,,,,,,,
MPTEMP,1,0
MPDATA,EX,1,,22.5E3          ! MPa 1 - Resina/Fibra de Vidro
MPDATA,EY,1,,11E3
MPDATA,EZ,1,,22.5E3
MPDATA,PRXY,1,,0.3
MPDATA,PRYZ,1,,
MPDATA,PRXZ,1,,
MPDATA,GXY,1,,6E+003
MPDATA,GYZ,1,,6E+003
MPDATA,GXZ,1,,6E+003


MPTEMP,,,,,,,,
MPTEMP,1,0
MPDATA,EX,2,,16              ! MPa  2 - Cortiça
MPDATA,PRXY,2,,0.01


MPTEMP,,,,,,,,
MPTEMP,1,0
MPDATA,EX,3,,22.5E3          ! MPa 3 - Resina/Fibra de Vidro
MPDATA,EY,3,,11E3
MPDATA,EZ,3,,22.5E3
MPDATA,PRXY,3,,0.3
```

```
MPDATA,PRYZ,3,,
MPDATA,PRXZ,3,,
MPDATA,GXY,3,,6E+003
MPDATA,GYZ,3,,6E+003
MPDATA,GXZ,3,,6E+003

MPTEMP,,,,,,,,
MPTEMP,1,0
MPDATA,EX,4,,16              ! MPa  4 - Cortiça
MPDATA,PRXY,4,,0.01



MPTEMP,,,,,,,,
MPTEMP,1,0
MPDATA,EX,5,,22.5E3          ! MPa 5 - Resina/Fibra de Vidro
MPDATA,EY,5,,11E3
MPDATA,EZ,5,,22.5E3
MPDATA,PRXY,5,,0.3
MPDATA,PRYZ,5,,
MPDATA,PRXZ,5,,
MPDATA,GXY,5,,6E+003
MPDATA,GYZ,5,,6E+003
MPDATA,GXZ,5,,6E+003

!*********************************************************************

!PONTOS:

K,1,
K,2,SIZE_SQ ,
K,3,H5,

K,4,L/2,

K,5,LT/2,
K,6,LT/2,H5,

K,7,L/2,H5,
```

K,8,H5,H5,
K,9,0,H5,
K,10,0,SIZE_SQ ,
K,11,SIZE_SQ ,SIZE_SQ ,

K,12,LT/2,H5+H4,

K,13,L/2,H5+H4,
K,14,H5,H5+H4,

K,15,0,H5+H4,

K,16,LT/2,H5+H4+H3,

K,17,L/2,H5+H3+H4,
K,18,H5,H5+H3+H4,

K,19,0,H5+H3+H4,
K,20,0,H5+H3+H2+H4,
K,21,H1,H5+H3+H4+H2,
K,22,L/2,H5+H3+H2+H4,
K,23,LT/2,H5+H3+H2+H4,
K,24,0,H5+H4+H3+H2+H1,
K,25,H1,H5+H4+H3+H2+H1,
K,26,L/2,H5+H4+H3+H2+H1,
K,27,LT/2,H5+H4+H3+H2+H1,

!PONTOS PARA ADICIONAR NOVO QUADRADO

K,28,0,SIZE_SQ1
K,29,SIZE_SQ1,SIZE_SQ1,
K,30,SIZE_SQ1,0,
K,31,SIZE_SQ1,SIZE_SQ1/2,
K,32,SIZE_SQ1/2,SIZE_SQ1,

K,33,SIZE_SQ1,H5+H4+H3+H2+H1,
K,34,SIZE_SQ1,H5+H4,
K,35,SIZE_SQ1,H5+H4+H3,
K,36,SIZE_SQ1,H5+H4+H3+H2,

!###

!LINES

L,1,2
L,2,3
L,3,4
L,4,5
L,5,6
L,7,6
L,8,7
L,9,8
L,10,9
L,1,10
L,10,11
L,11,8
L,2,11
L,3,8
L,4,7

L,6,12
L,7,13
L,8,14
L,9,15

L,13,12
L,14,13
L,15,14

L,12,16
L,13,17

L,14,18
L,15,19

L,17,16
L,18,17
L,19,18
L,19,20
L,20,24
L,24,25
L,20,21
L,18,21
L,25,26
L,26,27
L,26,22
L,17,22
L,17,16
L,16,23
L,23,27
L,22,23
L,21,22
L,21,25

!LINHAS QUANDO ADICIONADO O SEGUNDO QUADRADO

L,9,28
L,8,32
L,31,29
L,30,31
L,28,32
L,32,29
L,8,31
L,3,30
L,14,32
L,15,28
L,29,34
L,34,35
L,35,36

```
L,36,33
L,25,33
L,21,36
L,18,35
L,14,34
L,34,31
L,30,4
L,31,7
L,34,13
L,35,17
L,36,22
L,33,26

!##############################################

!AREAS

AL,1,13,11,10   ! SIZE_SQ
AL,2,14,12,13   ! TRAPEZIO DTO
AL,11,12,8,9   ! TRAPEZIO ESQ
AL,14,51,47,50  ! H5 ESQUERDA PEQUENA
AL,63,64,15,47          ! H5 ESQUERDA
AL,15,6,4,5     ! H5 DIREITA
AL,44,8,48,45   ! H4 ESQUERDA PEQUENA 1
AL,45,50,46,49  ! H4 ESQUERDA PEQUENA 2
AL,53,48,52,22  ! H4 ESQUERDA PEQUENA 3
AL,52,49,54,61  ! H4 ESQUERDA PEQUENA 4
AL,62,65,64,17  ! H4 ESQUERDA
AL,17,20,6,16   ! H4 DIREITA
AL,26,22,29,25  ! H3 ESQUERDA PEQUENA 1
AL,25,61,60,55  ! H3 ESQUERDA PEQUENA 2
AL,55,66,65,24  ! H3 ESQUERDA
AL,24,27,20,23  ! H3 DIREITA
AL,30,29,33,34  ! H2 ESQUERDA PEQUENA 1
AL,34,60,56,59  ! H2 ESQUERDA PEQUENA 2
AL,56,67,66,38  ! H2 ESQUERDA
AL,38,41,27,39  ! H2 DIREITA
AL,31,32,33,43  ! H1 ESQUERDA PEQUENA 1
```

```
AL,43,58,57,59  ! H1 ESQUERDA PEQUENA 2
AL,57,68,67,37  ! H1 ESQUERDA
AL,37,36,41,40  ! H1 DIREITA


/PNUM,KP,1
/PNUM,LINE,1
/PNUM,AREA,1

!#########################################################################
###


!MALHAS:

!MALHA
NDIV = 15
ESP = H5/NDIV  ! H5 É A ESPESSURA DO MAT DE BAIXO

! MALHA A1 SQUARE
KESIZE,1,SIZE_SQ/NDIV     ! SIZE_SQ É H5/3
KESIZE,2,SIZE_SQ/NDIV
KESIZE,11,SIZE_SQ/NDIV
KESIZE,10,SIZE_SQ/NDIV


!A2 E A3 AREAS TRAPEZOIDES

KESIZE,3,ESP ! OU SEJA ELEMT 3X MAIORES DO QUE SIZE_SQ.
KESIZE,8,ESP
KESIZE,9,ESP

KESIZE,14,2*ESP
KESIZE,15,2*ESP

! 0 - FREE MESHING; 1 - USE MAPPED MESHING

MSHAPE,0              ! 0 - USE QUADRILATERALS,  1 - USE TRIAGLES
```

```
MSHKEY,1                ! MAPPED

!MALHAR A1, A2 E A3
AATT, 5         !MATERIAL 5
AMESH,1         !MALHA QUADRADO A1
AMESH,2,3,1     !MALHA A2 E A3 AREAS TRAPÉZIOS

!MALHAR A4

LESIZE,50,,,10,2
LESIZE,51,,,10,2
AATT,5
AMESH,4

MSHKEY,0 !FREE MESH

!MALHAR A5

LESIZE,63,,,150,3
LESIZE,64,,,150,3

AATT, 5
AMESH,5

! MALHAR A6
LESIZE,4,,,100,3
LESIZE,6,,,100,3

AATT, 5
AMESH,6

!MALHAR A7
LESIZE,48,ESP
LESIZE,44,4*ESP
LESIZE,45,4*ESP
LESIZE,46,4*ESP

AATT, 4
```

```
AMESH,7

!MALHAR A8

LESIZE,49,,,10,2

AATT, 4
AMESH,8

!MALHAR A9

LESIZE,53,4*ESP
LESIZE,52,4*ESP
LESIZE,22,ESP

AATT, 4
AMESH,9

!MALHAR A10

LESIZE,61,,,10,2
LESIZE,54,4*ESP

AATT, 4
AMESH,10

!MALHAR A11 e A12

LESIZE,65,,,150,3
LESIZE,20,,,100,3

AATT, 4
AMESH,11,12,1

!MALHAR A13

LESIZE,29,ESP
LESIZE,26,4*ESP
```

```
LESIZE,25,4*ESP
AATT, 3
AMESH,13

!MALHAR A14

LESIZE,60,,,10,2
LESIZE,55,4*ESP
AATT, 3
AMESH,14


!MALHAR A17

LESIZE,33,ESP
LESIZE,30,6*ESP
LESIZE,34,6*ESP
AATT, 2
AMESH,17

!MALHAR A18

LESIZE,59,,,10,2
LESIZE,56,6*ESP
AATT, 2
AMESH,18

!MALHAR A21

LESIZE,32,ESP
LESIZE,31,H1/3
LESIZE,43,H1/3
AATT, 1
AMESH,21

!MALHAR A22

LESIZE,58,,,10,2
```

```
LESIZE,57,H1/3
AATT, 1
AMESH,22

!MALHAR A15 E A16
LESIZE,66,,,150,3
LESIZE,27,,,100,3
AATT, 3
AMESH,15,16,1

!MALHAR A19 E A20
LESIZE,67,,,150,3
LESIZE,41,,,100,3
AATT, 2
AMESH,19,20,1

!MALHAR A23 E A24
LESIZE,68,,,150,3
LESIZE,36,,,100,3
AATT, 1
AMESH,23,24,1


!#################################################################

! CONSTRAINS

DL,31, ,SYMM
DL,30, ,SYMM
DL,26, ,SYMM
DL,53, ,SYMM
DL,44, ,SYMM
DL,9, ,SYMM
DL,10, ,SYMM
DK,4,UY,0

!#################################################################
```

```
!LOADS

FK,24,FY,MAXLOAD/2



FINISH
/solu
SOLVE

FINISH
/POST1

PLDISP,2
```

Appendix 3 - Ansys Numerical FEM Model 2D – T3 Specimen's

```
/CLEAR,START
/PREP7


! T3 SPECIMEN


! VARIAVEIS

LT = 250                    !total length span
L = 160                     !length between the supports

MAXLOAD = -525.06 ! MAX LOAD SPECIMEN T3_NRX

! A - E

! 5F/1C/5F/1C/5F  TOTAL THICKNESS=8

H1 = 1.3375                     !5F  - Fibra Vidro (5 Camadas de 0.2675)

H2 = 2                      !1C  - Cork Core

H3 = 1.3375                 !5F  - Fibra Vidro (5 camadas de 0.2675)

H4 = 2                      !1C  - Cork Core

H5 = 1.3375                 !5  - Fibra Vidro (5 Camadas de 0.2675)


SIZE_SQ = H5/3  ! ESPESSURA DO MAT DE BAIXO / 3
SIZE_SQ1 = 2*H5 ! DOBRO DA ESPESSURA DO MAT DE BAIXO
```

```
! EL TYPE - 8 NOS
ET,1,PLANE183
!*

KEYOPT,1,3,3                    ! 0, TP, 2 - DP, 3 - PL STRESS W THICKNESS
R,1,20


!#########################################################################
#########


! MATERIAIS:



MPTEMP,,,,,,,,
MPTEMP,1,0
MPDATA,EX,1,,22.5E3          ! MPa 1 - Resina/Fibra de Vidro
MPDATA,EY,1,,11E3
MPDATA,EZ,1,,22.5E3
MPDATA,PRXY,1,,0.3
MPDATA,PRYZ,1,,
MPDATA,PRXZ,1,,
MPDATA,GXY,1,,6E+003
MPDATA,GYZ,1,,6E+003
MPDATA,GXZ,1,,6E+003


MPTEMP,,,,,,,,
MPTEMP,1,0
MPDATA,EX,2,,16              ! MPa  2 - Cortiça
MPDATA,PRXY,2,,0.01


MPTEMP,,,,,,,,
MPTEMP,1,0
MPDATA,EX,3,,22.5E3          ! MPa 3 - Resina/Fibra de Vidro
```

```
MPDATA,EY,3,,11E3
MPDATA,EZ,3,,22.5E3
MPDATA,PRXY,3,,0.3
MPDATA,PRYZ,3,,
MPDATA,PRXZ,3,,
MPDATA,GXY,3,,6E+003
MPDATA,GYZ,3,,6E+003
MPDATA,GXZ,3,,6E+003

MPTEMP,,,,,,,,
MPTEMP,1,0
MPDATA,EX,4,,16              ! MPa  4 - Cortiça
MPDATA,PRXY,4,,0.01



MPTEMP,,,,,,,,
MPTEMP,1,0
MPDATA,EX,5,,22.5E3          ! MPa 5 - Resina/Fibra de Vidro
MPDATA,EY,5,,11E3
MPDATA,EZ,5,,22.5E3
MPDATA,PRXY,5,,0.3
MPDATA,PRYZ,5,,
MPDATA,PRXZ,5,,
MPDATA,GXY,5,,6E+003
MPDATA,GYZ,5,,6E+003
MPDATA,GXZ,5,,6E+003

!########################################################################

!PONTOS:

K,1,
K,2,SIZE_SQ ,
K,3,H5,

K,4,L/2,

K,5,LT/2,
```

K,6,LT/2,H5,

K,7,L/2,H5,

K,8,H5,H5,
K,9,0,H5,
K,10,0,SIZE_SQ ,
K,11,SIZE_SQ ,SIZE_SQ ,

K,12,LT/2,H5+H4,

K,13,L/2,H5+H4,
K,14,H5,H5+H4,

K,15,0,H5+H4,

K,16,LT/2,H5+H4+H3,

K,17,L/2,H5+H3+H4,
K,18,H5,H5+H3+H4,

K,19,0,H5+H3+H4,
K,20,0,H5+H3+H2+H4,
K,21,H1,H5+H3+H4+H2,
K,22,L/2,H5+H3+H2+H4,
K,23,LT/2,H5+H3+H2+H4,
K,24,0,H5+H4+H3+H2+H1,
K,25,H1,H5+H4+H3+H2+H1,
K,26,L/2,H5+H4+H3+H2+H1,
K,27,LT/2,H5+H4+H3+H2+H1,

!PONTOS PARA ADICIONAR NOVO QUADRADO

K,28,0,SIZE_SQ1
K,29,SIZE_SQ1,SIZE_SQ1,
K,30,SIZE_SQ1,0,

K,31,SIZE_SQ1,SIZE_SQ1/2,
K,32,SIZE_SQ1/2,SIZE_SQ1,

K,33,SIZE_SQ1,H5+H4+H3+H2+H1,
K,34,SIZE_SQ1,H5+H4,
K,35,SIZE_SQ1,H5+H4+H3,
K,36,SIZE_SQ1,H5+H4+H3+H2,

!##

!LINES

L,1,2
L,2,3
L,3,4
L,4,5
L,5,6
L,7,6
L,8,7
L,9,8
L,10,9
L,1,10
L,10,11
L,11,8
L,2,11
L,3,8
L,4,7

L,6,12
L,7,13
L,8,14
L,9,15

L,13,12
L,14,13
L,15,14

L,12,16
L,13,17
L,14,18
L,15,19

L,17,16
L,18,17
L,19,18
L,19,20
L,20,24
L,24,25
L,20,21
L,18,21
L,25,26
L,26,27
L,26,22
L,17,22
L,17,16
L,16,23
L,23,27
L,22,23
L,21,22
L,21,25

!LINHAS QUANDO ADICIONADO O SEGUNDO QUADRADO

L,9,28
L,8,32
L,31,29
L,30,31
L,28,32
L,32,29
L,8,31
L,3,30
L,14,32
L,15,28

```
L,29,34
L,34,35
L,35,36
L,36,33
L,25,33
L,21,36
L,18,35
L,14,34
L,34,31
L,30,4
L,31,7
L,34,13
L,35,17
L,36,22
L,33,26

!###############################################

!AREAS

AL,1,13,11,10   ! SIZE_SQ
AL,2,14,12,13   ! TRAPEZIO DTO
AL,11,12,8,9   ! TRAPEZIO ESQ
AL,14,51,47,50  ! H5 ESQUERDA PEQUENA
AL,63,64,15,47          ! H5 ESQUERDA
AL,15,6,4,5     ! H5 DIREITA
AL,44,8,48,45   ! H4 ESQUERDA PEQUENA 1
AL,45,50,46,49  ! H4 ESQUERDA PEQUENA 2
AL,53,48,52,22  ! H4 ESQUERDA PEQUENA 3
AL,52,49,54,61  ! H4 ESQUERDA PEQUENA 4
AL,62,65,64,17  ! H4 ESQUERDA
AL,17,20,6,16   ! H4 DIREITA
AL,26,22,29,25  ! H3 ESQUERDA PEQUENA 1
AL,25,61,60,55  ! H3 ESQUERDA PEQUENA 2
AL,55,66,65,24  ! H3 ESQUERDA
AL,24,27,20,23  ! H3 DIREITA
AL,30,29,33,34  ! H2 ESQUERDA PEQUENA 1
AL,34,60,56,59  ! H2 ESQUERDA PEQUENA 2
```

```
AL,56,67,66,38  ! H2 ESQUERDA
AL,38,41,27,39  ! H2 DIREITA
AL,31,32,33,43  ! H1 ESQUERDA PEQUENA 1
AL,43,58,57,59  ! H1 ESQUERDA PEQUENA 2
AL,57,68,67,37  ! H1 ESQUERDA
AL,37,36,41,40  ! H1 DIREITA


/PNUM,KP,1
/PNUM,LINE,1
/PNUM,AREA,1

!#########################################################################
###


!MALHAS:

!MALHA
NDIV = 15
ESP = H5/NDIV  ! H5 É A ESPESSURA DO MAT DE BAIXO

! MALHA A1 SQUARE
KESIZE,1,SIZE_SQ/NDIV     ! SIZE_SQ É H5/3
KESIZE,2,SIZE_SQ/NDIV
KESIZE,11,SIZE_SQ/NDIV
KESIZE,10,SIZE_SQ/NDIV


!A2 E A3 AREAS TRAPEZOIDES

KESIZE,3,ESP ! OU SEJA ELEMT 3X MAIORES DO QUE SIZE_SQ.
KESIZE,8,ESP
KESIZE,9,ESP

KESIZE,14,2*ESP
KESIZE,15,2*ESP
```

```
! 0 - FREE MESHING; 1 - USE MAPPED MESHING

MSHAPE,0              ! 0 - USE QUADRILATERALS,  1 - USE TRIAGLES
MSHKEY,1              ! MAPPED

!MALHAR A1, A2 E A3
AATT, 5        !MATERIAL 5
AMESH,1       !MALHA QUADRADO A1
AMESH,2,3,1     !MALHA A2 E A3 AREAS TRAPÉZIOS

!MALHAR A4

LESIZE,50,,,10,2
LESIZE,51,,,10,2
AATT,5
AMESH,4

MSHKEY,0 !FREE MESH

!MALHAR A5

LESIZE,63,,,150,3
LESIZE,64,,,150,3

AATT, 5
AMESH,5

! MALHAR A6
LESIZE,4,,,100,3
LESIZE,6,,,100,3

AATT, 5
AMESH,6

!MALHAR A7
LESIZE,48,ESP
LESIZE,44,4*ESP
LESIZE,45,4*ESP
```

```
LESIZE,46,4*ESP

AATT, 4
AMESH,7

!MALHAR A8

LESIZE,49,,,10,2

AATT, 4
AMESH,8

!MALHAR A9

LESIZE,53,4*ESP
LESIZE,52,4*ESP
LESIZE,22,ESP

AATT, 4
AMESH,9

!MALHAR A10

LESIZE,61,,,10,2
LESIZE,54,4*ESP

AATT, 4
AMESH,10

!MALHAR A11 e A12

LESIZE,65,,,150,3
LESIZE,20,,,100,3

AATT, 4
AMESH,11,12,1

!MALHAR A13
```

```
LESIZE,29,ESP
LESIZE,26,4*ESP
LESIZE,25,4*ESP
AATT, 3
AMESH,13

!MALHAR A14

LESIZE,60,,,10,2
LESIZE,55,4*ESP
AATT, 3
AMESH,14


!MALHAR A17

LESIZE,33,ESP
LESIZE,30,6*ESP
LESIZE,34,6*ESP
AATT, 2
AMESH,17

!MALHAR A18

LESIZE,59,,,10,2
LESIZE,56,6*ESP
AATT, 2
AMESH,18

!MALHAR A21

LESIZE,32,ESP
LESIZE,31,H1/3
LESIZE,43,H1/3
AATT, 1
AMESH,21
```

```
!MALHAR A22

LESIZE,58,,,10,2
LESIZE,57,H1/3
AATT, 1
AMESH,22

!MALHAR A15 E A16
LESIZE,66,,,150,3
LESIZE,27,,,100,3
AATT, 3
AMESH,15,16,1

!MALHAR A19 E A20
LESIZE,67,,,150,3
LESIZE,41,,,100,3
AATT, 2
AMESH,19,20,1

!MALHAR A23 E A24
LESIZE,68,,,150,3
LESIZE,36,,,100,3
AATT, 1
AMESH,23,24,1


!#####################################################################

! CONSTRAINS

DL,31, ,SYMM
DL,30, ,SYMM
DL,26, ,SYMM
DL,53, ,SYMM
DL,44, ,SYMM
DL,9, ,SYMM
DL,10, ,SYMM
DK,4,UY,0
```

```
!#####################################################################

!LOADS

FK,24,FY,MAXLOAD/2



FINISH
/solu
SOLVE

FINISH
/POST1

PLDISP,2
```